ESTIMATING RATES OF EXCHANGE ACROSS THE SEDIMENT/WATER
INTERFACE IN THE LOWER MERCED RIVER, CA

Celia Zamora
B.S., Evergreeen State College, Olympia, WA, 1997

THESIS

Submitted in partial satisfaction of
the requirements for the degree of

MASTER OF SCIENCE

in

GEOLOGY

at

CALIFORNIA STATE UNIVERSITY, SACRAMENTO

SPRING
2006

ESTIMATING RATES OF EXCHANGE ACROSS THE SEDIMENT/WATER
INTERFACE IN THE LOWER MERCED RIVER, CA

A Thesis

By

Celia Zamora

Approved by:

_____, Committee Chair
Timothy C. Horner

_____, Second Reader
David G. Evans

_____, Third Reader
Charles R. Kratzer

Date:_____

Student: __Celia Zamora__

I certify that this student has met the requirements for format contained in the University format manual, and that this thesis is suitable for shelving in the Library and credit is to be awarded for the thesis.

_____ _____

Timothy C. Horner, Committee Chair   Date
Department of Geology

Abstract

of

ESTIMATING RATES OF EXCHANGE ACROSS THE SEDIMENT/WATER
INTERFACE IN THE LOWER MERCED RIVER, CA

By

Celia Zamora

Abstract: The lower Merced River Basin was chosen by the U.S. Geological Survey's (USGS) National Water Quality Assessment Program (NAWQA) to participate in a national study on how hydrological processes and agricultural practices interact to affect the transport and fate of agricultural chemicals. As part of this effort, surface-water/ground water (sw/gw) interactions have been studied in an instrumented 100 m reach on the lower Merced River. This thesis project focused on estimating vertical rates of exchange across the sediment/water interface by direct measurement using seepage meters and by using temperature as a tracer coupled with numerical modeling. High-precision temperature loggers and pressure transducers were placed within the streambed and in the river to continuously monitor temperature and hydraulic head every 15 minutes from March 2004 through October 2005. One-dimensional modeling of heat and water flow was used to interpret the temperature and head observations and deduce the sw/gw fluxes using a USGS numerical model, VS2DH, which uses an energy transport approach via the advection-dispersion equation. Results of the modeling efforts indicate that the Merced River at the study reach is generally a slightly gaining stream with small head differences (cm) between the surface water and ground water with flow reversals occurring during high streamflow events. The average vertical flux across the sediment/water interface was 0.4-2.2 cm/day and the range of hydraulic conductivities was 1-3 m/day. Seepage meters generally failed in this high-energy system due to slow seepage rates and a moving streambed resulting in scour or burial of the seepage meters. Estimates of streambed hydraulic conductivity were also made by grain size analysis methods and slug tests.

_____, Committee Chair
Timothy C. Horner

ACKNOWLEDGEMENTS

TABLE OF CONTENTS

LIST OF FIGURES

LIST OF TABLES

INTRODUCTION

Hydrologists traditionally regarded streams and ground water as distinct, independent resources to be utilized and managed separately. However, with increased demands on water supplies, hydrologists realized that streams and ground water are parts of a single, interconnected resource (Winter and others, 1998).   Attempts to distinguish these resources for analytical or regulatory purposes often meet with difficulty because sustained depletions of one resource negatively impact the other. An understanding of the interconnections between surface water and ground water is therefore essential. Scientists have begun to show that local hydrologic interactions between surface water and ground water play an important role in stream ecosystem structure and function (Gilbert and others., 1994; Findlay, 1995; Brunke and Gonser, 1997). Water that passes back and forth between the surface water and subsurface water influences the fate and mobilization of trace metals and organic pollutants, and can enhance biogeochemical reactions that can affect downstream water quality. Understanding these interactions at small scales requires knowledge of ground water flow paths and their linkages to streams, rates of exchange between stream and ground water systems, and the mechanisms that generate spatial (channel unit, reach, and watershed) and temporal (diel, seasonal) variations in these processes (Wroblicky, and others, 1998). Rates of exchange across a streambed are most commonly estimated using one or more of the following approaches: (1) Darcy ground water flux calculations, (2) tracer based approaches and (3) direct measurements across a streambed using a device such as a seepage meter. The Darcy

approach calculates water fluxes across streambeds on the basis of two dimensional maps of hydraulic head, estimates of hydraulic conductivity of near-channel sediment, and the basic governing equations for ground water flow (Harvey and Wagner, 2000). The tracer approach observes an introduced tracer (ie. salt, deionized water, bromide) or an environmental tracer (temperature or specific conductance) to infer flux rates across the streambed. A seepage meter directly measures vertical flux across the sediment/water interface

Background

The Merced River, located in the San Joaquin River Basin in central California was chosen by the U.S. Geological Survey (USGS) National Water Quality Assessment (NAWQA) Program as one of five study areas in a national study on how hydrological processes and agricultural practices interact to affect the transport and fate of agricultural chemicals in nationally important agricultural settings. Key to achieving this objective is an understanding of how the agricultural chemicals move through each hydrologic compartment, as well as estimating rates of exchange between compartments. Five hydrologic compartments were monitored: the atmosphere, surface water, the unsaturated zone, ground water, and the hyporheic zone (surface water – ground water interaction). This project focused on estimating rates of exchange between the surface water and ground water across the sediment/water interface in the lower Merced River, California.

Study Objective

The objective of this study is to estimate rates of exchange across the sediment/ water interface in a 100 meter reach of the Merced River, California. The tracer based approach and direct measurement across the streambed using seepage meters were used to meet the study objective. Temperature was considered a tracer and precision temperature logging devices recorded temperature (°C) at specified depths and locations within the streambed and in the adjacent riparian zone at two instrumented transects. The temperature loggers were used to record the movement of ground water into the stream, or conversely the movement out of the stream and therefore monitored the surface water/ ground water (sw/gw) exchanges throughout the study period. Pressure transducers located in-stream and below the streambed collected water level data that were used to define boundary conditions. The collected temperature and pressure head data were input into a USGS numerical model, Variably Saturated 2-Dimensional Heat (VS2DH) that used an energy transport approach by way of the advective-dispersion equation to simulate heat and flow transport (Healy and Ronan, 1996). Estimates of streambed hydraulic and thermal conductivity were input into the model until model simulations "best fit" observed streambed temperatures at depth. Direct measurement of flux was measured using seepage meters and results were compared to flux rates obtained through the modeling results. Estimates of the hydraulic conductivity of streambed sediments were also approximated from the results of sieve tests analysis conducted on samples collected from the streambed and slug tests.

Study Area

The study area is located in the lower Merced River Basin which lies on the east side of the San Joaquin Valley in the San Joaquin Basin and is approximately 831 square kilometers (figure 1). The lower Merced Basin is predominately agricultural on the valley floor and lies within the flat structural basin of the San Joaquin Valley. The upstream side of the basin extends eastward into the lower foothill of the Sierra Nevada. The San Joaquin Valley is bounded by the Sierra Nevada to the east, the Coast Ranges to the west, the Tehachapi Mountains to the south, and the Sacramento-San Joaquin Delta to the north. The boundary of the basin is defined by the topographic drainage divides and in some areas, by canals and lateral that serve this area. Altitude ranges from 22 meters in the San Joaquin Valley to 168 m above sea level in the Sierra Nevada foothills. Elevation gradients average about 2.5 meters/kilometer on the valley floor and 26.7 meters/kilometer in the foothills (J.M. Gronberg, USGS, written communication, 2006). Approximately 55 percent of the lower Merced River Basin is covered by agricultural land, 39 percent is forest, shrub-land, and grassland, over 4 percent is urban and transitional land, and less than 2 percent is water and wetland (Vogelmann and others, 2001). The forest, shrub land, and grassland are predominantly on the valley floor.
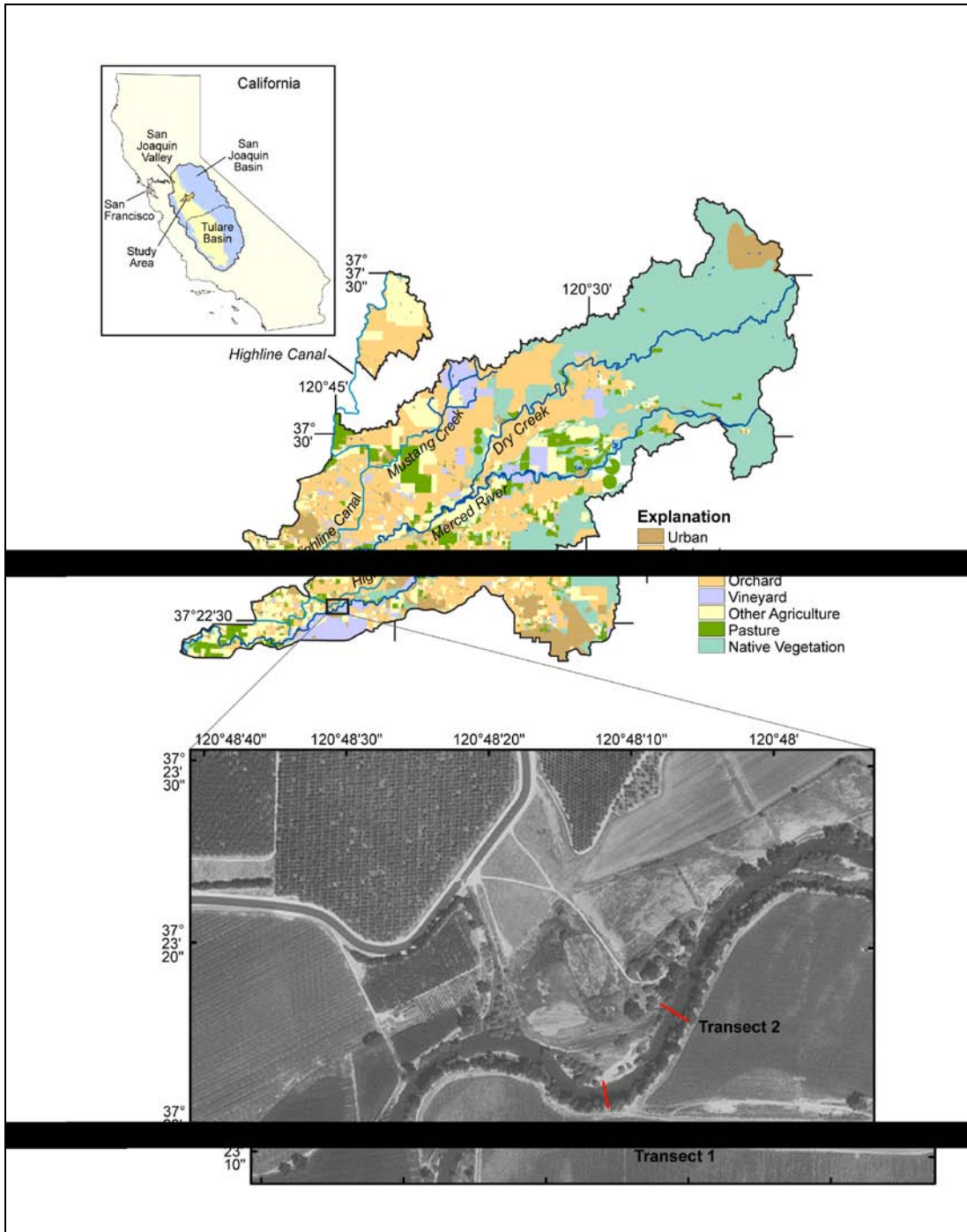
Figure 1. Study area and location of fixed transect 1 and transect 2 located within the Lower Merced Basin.

Geology

The San Joaquin Valley is part of the Central Valley, which is a large, northwest-trending, asymmetric structural trough, filled with marine and continental sediments (Bartow, 1991). To the east of the valley, the Sierra Nevada is composed primarily of pre-Tertiary granitic rocks and is separated from the valley by a foothill belt of marine and metavolcanic rocks. The Coast Ranges west of the valley are a complex assemblage of rocks, including marine and continental sediments of Cretaceous to Quaternary age (Page, 1977; Page 1986). Alluvial deposits of the eastern part of the valley were derived primarily from the weathering of granitic instrusive rocks of the Sierra Nevada and are highly permeable, medium- to coarse- grained sands with low total organic carbon, forming broad alluvial fans where the streams enter the valley. These deposits generally are coarsest near the upper parts of the alluvial fans and finest near the valley trough. Dune sand, derived from the alluvial deposits, consists of well-sorted medium-to-fine sand, as much as 43 meters thick (Page, 1986). Stream- channel deposits along the Merced River consist of medium to coarse sand.

Consolidated rocks and deposits exposed along the margin of the valley floor include Tertiary and Quaternary continental deposits, Cretaceous and Tertiary marine sedimentary rocks, and the pre-Tertiary Sierra Nevada basement complex (Davis and Hall, 1959; Croft, 1972; Page and Balding, 1973). The majority of the unconsolidated deposits in the study area are contained within the Pliocene-Pleistocene Laguna, Turlock Lake, Riverbank, and Modesto Formations, with minor amounts of Holocene stream channel and flood-basin deposits. The Turlock Lake, Riverbank, and Modesto

Formations form a sequence of overlapping channel incision that were influenced by climatic fluctuations, and resultant glacial stages in the Sierra Nevadas (Bartow, 1991).

The Corcoran Clay, at the base of the upper Turlock Lake Formation, is a lacustrine deposit that is a key subsurface feature in the San Joaquin Valley. Page (1986) mapped the areal extent of this regional aquitard based on a limited number of well logs and geophysical logs. Additional lithologic data recently were used to modify the extent of this important unit (Burow and others, 2004). The eastern extent of the Corcoran Clay roughly parallels the San Joaquin River valley axis. The Corcoran Clay ranges in depth from 28 to 85 meters below land surface and a thickness from 0 to 57 meters in the study area.

Climate

The San Joaquin Valley has an arid-to-semiarid climate that is characterized by hot summers and mild winters. Average temperatures are fairly uniform over the valley floor. Temperature decreases with increasing elevation in the foothills and mountains of the Sierra Nevada. Long-term records for temperature do not exist for sites within the lower Merced River Basin. However, Modesto Irrigation District (MID) has temperature data for downtown Modesto for 1939 to 2005 (Modesto Irrigation District, 2005). Mean low temperatures in degrees F range from mid 30's in the winter months to upper 50's in the summer. Mean high temperatures in degrees F range from mid 50's in the winter months to mid 90's in the summer (J.M. Gronberg, USGS, written communication, 2006). As with temperature, long-term precipitation records do not exist within the lower

Merced River Basin. However, MID does have long-term precipitation record for Modesto for 1889 to 2005. Mean annual precipitation (1889-2005) in Modesto is 31 centimeters, but annual precipitation is highly variable. Eighty percent of the precipitation falls during November through March, with the maximum precipitation in December through February.

<u>Surface Water Hydrology</u>

The surface-water hydrology of the Merced River Basin has been significantly modified by the development of water resources. Between the 1870's and the early 1900's, miles of canals were constructed to convey water to the land. Exchequer Dam was completed in 1926 to provide flood control and water for irrigation and power generation. In 1967, New Exchequer Dam was completed to expand Lake McClure Reservoir capacity to 1.26 cubic kilometers. In the same year, McSwain Dam was completed downstream as a regulating reservoir. Downstream of McSwain Dam, the Merced Falls Dam diverts flow into the Merced Irrigation District Northside Canal to provide irrigation water to areas north of the Merced River. Further downstream, Crocker-Huffman Dam diverts flow into the Merced Irrigation District Main Canal (Stillwater Sciences and EDAW, 2001). The area of focus for this study, the lower Merced River Basin, starts at New Exchequer Dam. Water quality above this point for the most part is unaffected by agricultural activities. The lower Merced River receives water from Dry Creek, and Mustang Creek by way of Highline Canal.

Mean annual streamflow measured at the California Department of Water Resources (CDWR) Merced River near Stevinson gaging station (24 kilometers downstream of the study site) is approximately 19.6 m^3/s for water years 1941-2005. Mean annual streamflow for this time period varies greatly from year to year. Recent water years, 2003-2004, had below normal streamflow, whereas 2005 saw above average streamflow due to above average snowpack in the Sierras above Exchequer Dam (figure. 2). In a natural basin, the usual trend is to see higher streamflow downstream as the area of contribution increases. However, because the Merced River is highly engineered and utilized for agricultural irrigation it shows an overall decrease in streamflow from the upper basin to the mouth.
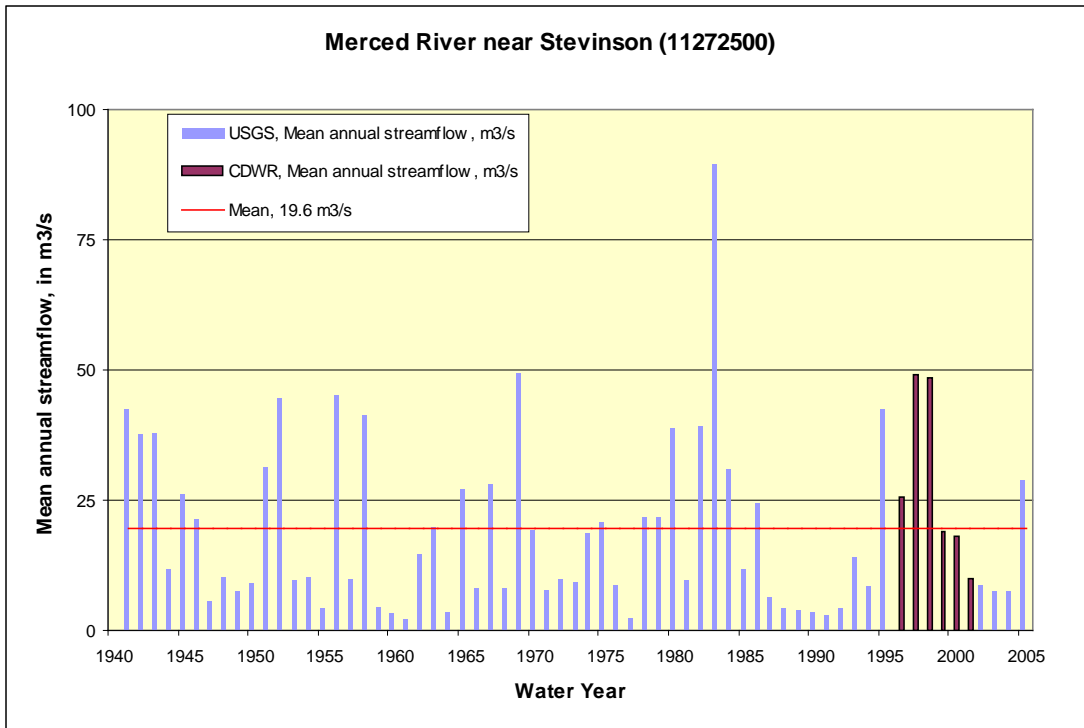
Figure 2. Mean annual streamflow, Merced River near Stevinson, California, water years 1941-2005

Ground Water Hydrology

Ground water occurs primarily in the unconfined to semiconfined aquifer above and east of the Corcoran Clay and in the confined aquifer beneath the Corcoran Clay. The unconfined to semi-confined aquifer above the Corcorran Clay ranges in thickness from about 40 to 70 meters. The unconfined to semi-conconfined east of the Corcorran Clay is composed primarily of alluvial sediment, but includes the upper part of the Mehrten Formation, which is more consolidated than the overlying formations. The confined aquifer is composed of alluvial sediments and upper Mehrten Formation sediments from beneath the Corcorran Clay to the base of fresh water (S. Phillips, USGS, written communication, 2006).

Under natural conditions, ground water recharge was primarily at the upper parts of the alluvial fans from streams entering the valley. Most ground water was discharged as evapotranspiration in the central trough of the valley, and to a lesser extent, to streams. Ground-water resource development in the basin changed the ground-water flow regime. Pumping for agricultural irrigation and irrigation return flows are much greater than natural recharge and discharge and caused and increase in vertical flow in the system. Ground-water flow is generally toward the southwest and is somewhat similar to the pre-development flow regime (J.M. Gronberg, USGS, written communication, 2006). However, ground water moving along a horizontal flow path is extracted by wells and reapplied at the surface several times before reaching the valley trough (S. Phillips, USGS, written communication, 2006).

DIRECT MEASUREMENT OF VERTICAL FLUX

The seepage meter allows direct measurement of seepage flux across the sediment-water interface. It consists of a bottomless cylinder formed from an inverted drum or bucket, connected to a collection bag by a length of tubing. The device is pushed into the bed of a lake or stream and a collection bag with a known volume of water is attached. The collection bag is then removed after a period of elapsed time and the rate of vertical ground water flux through the area enclosed by the seepage meter is calculated from the increase or decrease in the initial volume of water, the length of time elapsed and the area of the seepage meter. Flux rates are obtained as length/time. An increase in the initial volume indicates a positive vertical flux rate (ground water to surface water), and a decrease in initial volume indicates a negative vertical flux rate (surface water to ground water).

Review of Literature

The seepage meter was initially developed to measure losses from irrigation canals (Israelson and Reeve, 1944) and in the mid-1970's the design was improved and the use was expanded to measure ground water discharge into lakes (Lee, 1977; Lee and Cherry, 1978; John and Lock, 1977; Connor and Belanger, 1981; Erickson, 1981;Woessner and Sullivan, 1984; Isiorho and Matisoff, 1990; Shaw and Prepas, 1990b; Lesack, 1995; Rosenberry, 2000; Sebestyn and Schneider, 2001). Because seepage meters provide a quick and simple method for gathering information on the direction, rate, and variability

and seepage flux across the sediment-water interface, their use has been expanded to environments other than lakes. Vertical seepage rates have been measured in wetlands (Choi and Harvey, 2000), estuaries (Lee, 1977; Lock and John, 1978; Zimmerman and others, 1985; Yelverton and Hackney, 1986; Boyle, 1994; Linderfelt and Turner, 2001), and nearshore ocean margins (Cable and others, 1997; Shinn and others, 2002; Taniguchi, 2002; Chanton and others, 2003). Seepage meters have also been used to determine water budgets (Fellows and Brezonik, 1980), or obtain samples for chemical analysis (Lee, 1977; Downing and Peterka, 1978; Brock and others, 1982; Belander and Mikuntel, 1985; Shaw and others, 1990).

A growing interest in investigating the rates of exchange between streams and ground water has led to the use of seepage meters in stream channels (Lee and Hynes, 1977; Connor and Belanger, 1981; McBride, 1987; Libelo and MacIntyre, 1994; Blanchefield and Ridgeway, 1996; Jackman and others, 1997; Cey and others, 1998; Fryer and others 2000; Dumouchelle 2001; Landon and others, 2001; Murdoch and Kelly, 2003). However, the data obtained are often highly variable because the original design and application was intended for lake and estuary environments. Flume and laboratory studies show that much of this variation is due to the effects of flow across the seepage meter collection bag, which alters the hydraulic head within the meter and induces seepage flow (Libelo and MacIntrye, 1994). Their study discovered that the induced seepage flow can be significantly reduced by isolating the seepage meter collection bag from the stream flow.

Concerns over the effects that size, thickness and initial conditions of the attached collection bag have on measured seepage rates have prompted investigations in field and laboratory settings. Shaw and Prepas (1989) found that an anomalous, short-term influx of water into seepage meters occurred immediately after connecting the collection bag to the seepage meter, but showed that the anomaly could effectively be eliminated by attaching pre-filled collection bags with a minimum of 1000 ml before attaching to the seepage meter. The effects of bag type and meter size on seepage meter measurements where evaluated in a laboratory setting by Isiorho and Meyer (1999). Their study found that there was no significant difference due to bag type, but found that smaller diameter seepage meters had a greater variance. Laboratory studies have also examined bag conductance, the ratio of the volumetric flow rate into the bag to the hydraulic head required to fill the bag (Murdoch and Kelly, 2003). Harvey and Lee (2000) found that the conductance of a bag formed from a thin compliant film is expected to be large and relatively constant until it is filled with enough water to cause stretching, at which point it will decrease. The conductance of a bag may also vary if the bag deforms in an irregular manner and will decrease if kinks or folds develop in the bag (Kelly, 2001). As a collection bag opens and approaches its manufactured shape a gradual decrease in conductance of the bag with increasing volume was observed by Schincariol and McNeil (2002). Similar results were observed by Shaw and Prepas (1989) and Blanchfield and Ridgeway (1996).

In field settings, slow seepage rates and the relatively small area measured also present problems. Very slow seepage rates may require a meter to be in place for several days. The problem of measurement area is of concern because most researchers and watershed managers are interested in seepage processes on a scale of hundreds to thousands of m^2 or more, and most seepage meters typically integrate vertical flux over an area of approximately 0.25 m^2 or less (Rosenberry, 2005). Rosenberry addressed these issues in a low permeability zone by connecting multiple seepage meter cylinders together to a single collection bag to increase the area represented by each measurement, thus integrating spatial heterogeneity over a larger area, and reducing the time required to collect a measurable change in volume.

Some investigators (Erickson, 1981; Brock and others, 1982; Woessner and Sullivan, 1984; Shaw and Prepas, 1990a; Blanchfield and Ridgeway, 1996; Harvey and Lee, 2000) using seepage meters have expressed guarded concerns that the performance of the meter itself may cause variability that is unrelated to, and can obscure, the natural processes that they are trying to characterize (Schincariol and McNeil, 2002). Erickson (1981) stated that seepage meters disturb the flow field in which they are installed, resulting in consistently lower measured seepage rates. This disturbance is apparently related to frictional resistance along the internal boundaries of the meter. Frictional resistance is inherent to some extent in all in all seepage meter designs, and as a result, several laboratory studies have come up with a seepage meter coefficient that is used to convert measured seepage rates to true values. Coefficients in the literature range from 1.1 to 1.7 (Erickson, 1981; Cherkauer and McBride, 1988; Asbury 1990; Belanger and

Montgomery, 1992). Many of the less-efficient meter designs require larger coefficients, primarily because they use small-diameter tubing to connect the bag to the seepage cylinder (Rosenberry, 2005). The use of large-diameter plumbing greatly reduces loss of efficiency, resulting in a smaller correction coefficient (Fellows and Brezonik, 1980; Rosenberry, 2005).

Murdoch and Kelly (2003) developed a theoretical analysis to evaluate the extent to which bag conductance and velocity head may affect flux measurements by a seepage meter. Their analysis showed that bag conductance, radius of the seepage meter, and hydraulic conductivity of the streambed can be combined to give a dimensionless term that characterizes seepage meter performance. Some seepage meters use electronic flowmeters (Paulson and others, 2001; Taniguchi and Fukuo, 1993; Rosenberry and Morin, 2004) to eliminate problems encountered with the collection bag. Although these devices show promise, their availability and expense make their use limited. This study focused on the conventional seepage meter that is both inexpensive and easily fabricated.

The purpose of using seepage meters to directly measure seepage rates was to gain an overall understanding of the direction, rate, and variability of seepage rates within the study area and compare these results to modeled flux rates that use temperature as a tracer. The direct measurement methods and design of the seepage meter used in this study incorporated suggestions made by investigators (Libelo and MacIntrye, 1994; Shaw and Prepas, 1989; Kelly, 2001; Murdoch and Kelly, 2003) in an attempt to minimize variability in measured vertical seepage rates. Additionally, the performance of the collection bags used in this study was examined under controlled gradients in a

laboratory test tank. As a result, improvements were made to the seepage meters and collection bags following these laboratory tests. The field and laboratory methods and results are discussed separately.

Field Measurements

<u>Field Methods</u>

Flux rates across the sediment-water interface were measured directly using a total of twelve drum-style (Lee, 1977) seepage meters. Two sizes of seepage meters were used: the larger meters were 2500 cm^2 in cross-sectional area by 26.5 cm deep and the smaller meters were 620 cm^2 in cross-sectional area by 13.5 cm deep. The field deployment methods for both sizes of meters was to carefully push each meter into the riverbed sediment leaving approximately 5 cm of the top of each meter above the streambed bottom. The deployment array of the seepage meters placed in the streambed involved pairing a large and small seepage meter spaced approximately 1.5 meters apart. The purpose of pairing the meters was to compare flux rates between seepage meter pairs and observe variability in measured rates for the same size meter over consecutive measurements. Two deployment arrays were used throughout the study. The first deployment array involved placing the six paired meters perpendicular to flow across two transects separated by a distance of approximately 10 meters, and the second deployment array placed the paired meters across two transects separated by a distance of approximately 100 meters (figure 3). The seepage meter pairs depicted in these figures will be referred to as A-1, B-2, C-3, etc., hereinafter.
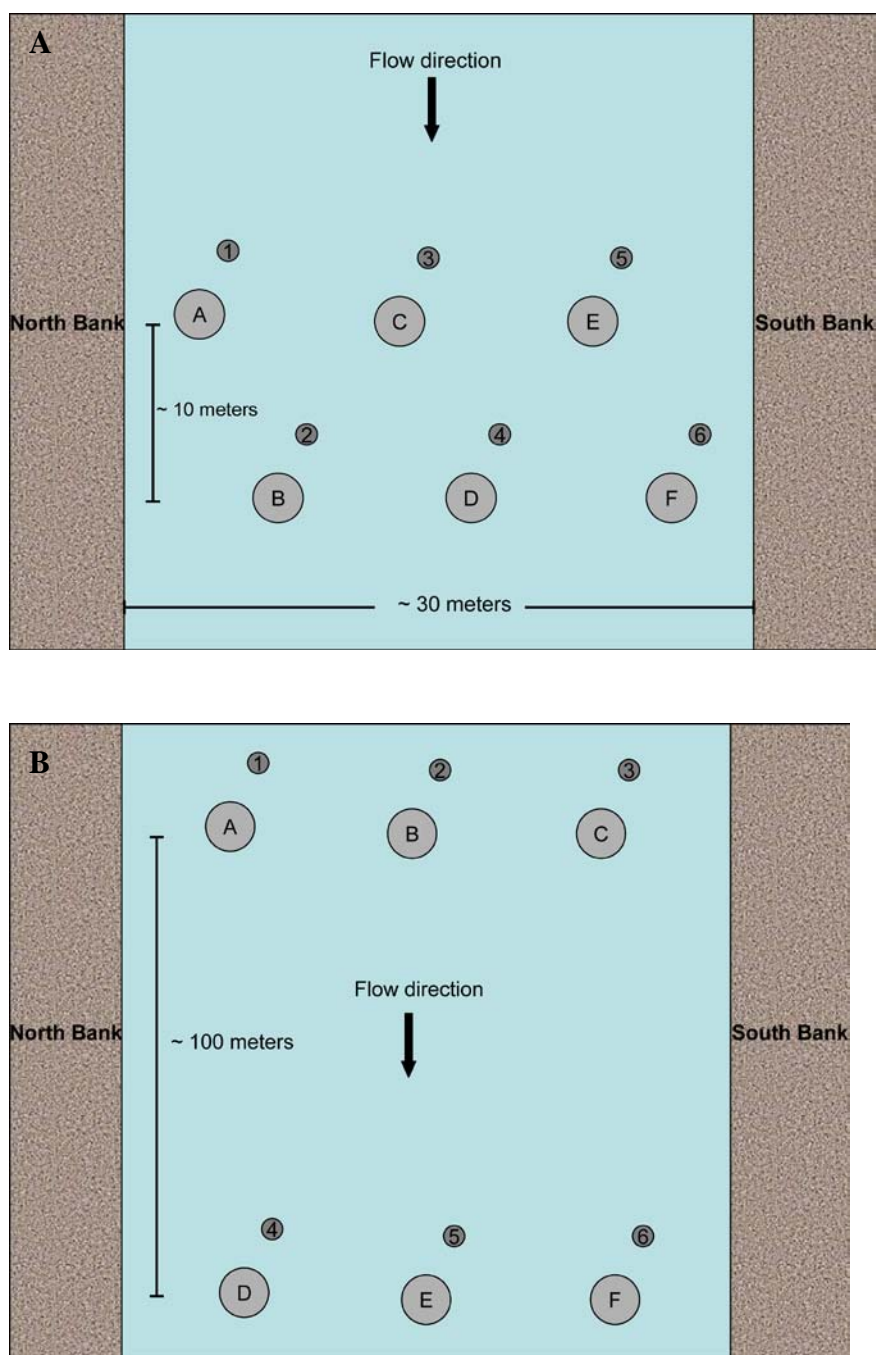
Figure 3.   Seepage meter arrays. (**A**) array one. (**B**) array two

The meters were then left undisturbed for 12 to 24 hours to allow trapped air to escape, as well as permit riverbed sediments to return to equilibrium after being disturbed during installation. Once deployed, the meters were left in place for the duration of the measuring event. Following the equilibration period, the collection bags were pre-filled with 500 - 1000 ml of water and placed in housing units to protect the bag from the current of the river and connected to the seepage meters. The collection bags and housing units were connected to the seepage meters using a 61cm length of 0.64-cm-i.d. vinyl tubing. The housing unit for the large seepage meter was a perforated Rubbermaid® storage box that was secured to the top of the seepage meter with a bungee cord. The small seepage meter used the half of a drum as the housing unit for the collection bag and was simply pushed into the sediment alongside the seepage meter (figures 4 and 5).

Careful attention was given to avoid disturbing the sediments around each of the paired meters, and the attachment and retrieval of collection bags was done by snorkeling to and from each meter to eliminate any contact with the riverbed bottom. Due to the slow flux rates encountered, the collection bags were retrieved and redeployed approximately every 12-24 hours over a period of a few days. The change in volume was either measured using a graduated cylinder or weighed with a scale, and the elapsed time was recorded. The change in volume (ml/min) over the elapsed time (days) was divided by the cross-sectional area of the seepage meter (cm^2) to obtain vertical flux rates in cm/day.

Figure 4. Large seepage meter with attached housing unit (left) and small seepage meter with housing unit (right).

Figure 5. Field deployment of paired seepage meters.

Three types of collection bags were used in the study. The collection bag types used were a 1800 ml Sun Shower Solar Bag [®], a 2000 ml medical urine collection bag, and a 2000 ml Void-Fill[®] packaging bag. These collection bags will be referred to as shower bag, medical bag and packaging bag, respectively. Initial field measurements used only the shower and medical collection bags attached to the large and small seepage meters, respectively. However, the results of laboratory test runs prompted exclusive use of the packaging collection bag in seepage rate measurements made in the latter part of the study. Also, the fittings for the large seepage meter were changed to a barbed nipple to reduce head loss observed in the laboratory test runs with the previous connection device. The performance and results of each of the collection bags is presented in the laboratory methods section.

A total of six sampling events were made over a period of ten months beginning in December 2003 and ending in September 2004. The period of time given to each field measurement period was initially intended to be one week. However, stream scour around the seepage meters resulted in only 2-3 repeat measurements taken over a 48-72 hour period. Because improvements were made to the seepage meter and collection bags over the period of the study, the objective and methods of each field visit are discussed individually. Table 1 lists the sampling objective, seepage meter array, bag types and flow conditions for each sampling event.

Table 1. Objective of field measurements using seepage meters

Field Measurement Period	Flow Velocity (m/s)	Approximate Depth (m)	Seepage Meter Array	Seepage Meter size	Bag type	Objective
February 11-12, 2004	0.67	0.78	1	large	shower bag	compare seepage rates between bag types and paired meters
				small	medical bag	
July 20-21, 2004	0.65	0.76	1	large	shower bag	compare measured rates using shower and medical bags in first 24 hour period to
				small	medical bag	
July 21-22, 2004			1	large	packaging bag	measured rates using only packaging bags in second 24 hour period
				small	packaging bag	
September 21-22, 2004	0.71	0.91	1	large	shower bag	compare measured rates using shower and medical bags in first 24 hour period to
				small	medical bag	
September 22-23, 2004			1	large	packaging bag	measured rates using only packaging bags in second 24 hour period
				small	packaging bag	
September 23-24, 2004	0.27	0.58	2	large	packaging bag	compare measured rates between repeat measurements using same bag type and compare measured rates between seepage meters
				small	packaging bag	
December 1-4, 2003			2	large	packaging bag	
				small	packaging bag	
January 28-29, 2004	0.38	0.79	2	large	packaging bag	compare measured rates between repeat measurements using same bag type and compare measured rates between seepage meters
				small	packaging bag	
January 29-30, 2004			2	large	packaging bag	
				small	packaging bag	
February 10-11, 2004				large	packaging bag	
				small	packaging bag	

Field Results

The initial intention of the seepage meter for this study was to use a simple device to gain an overall understanding of the magnitude, direction, and variability of seepage rates across the sediment-water interface in the Merced River; however problems encountered with the streambed sediments proved to be significant. In the area of study, the streambed of the Merced River is relatively flat and primarily made up of medium to coarse-grained homogeneous eolian sand. It was assumed at the beginning of the study that the use of seepage meters at this site would not encounter the spatial variability problems that are often encountered when using seepage meters in heterogeneous sediments. It was also expected that the flux rates would be roughly uniform and give an indication as to whether the study area was gaining or losing. These assumptions proved to be incorrect. Variability in measurements was encountered between seepage meter pairs in both direction and magnitude as well as in the repeat measurements made for the same seepage meter in a given 24 hour period.

Observations of the streambed during site visits revealed that the stream bottom is continually moving─ small dunes would develop and hours later would disappear. The problem was further compounded by the slow seepage rates, which required the seepage meters to be in place for several days and be subjected to the moving streambed resulting in scour at the base of the meter(s) (figure 6). Scoured-out seepage meters took in river water and filled the collection bag to maximum capacity, resulting in erroneously high seepage rates.   In addition, the housing unit for the small seepage meter was not as effective as the housing unit for the large seepage meter.

flow direction
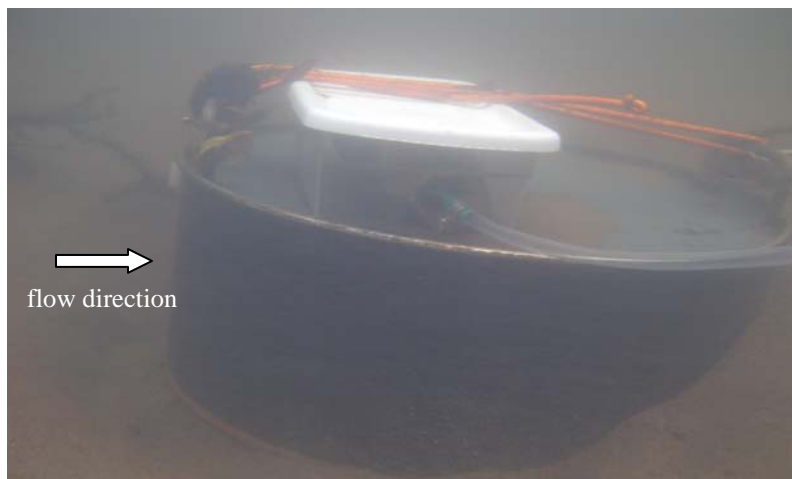
Figure 6. Scouring out of seepage meter typically encountered 48 hrs. after deployment

The housing units would scour out, become dislodged, and subject the collection bag to the flow of the river, thereby inducing volumetric flow into the collection bag. In other cases, the housing unit would become buried under the streambed sediments resulting in complete loss of initial volume.

The original intent of pairing the seepage meters to compare flux rates between the two sizes gave variable results. In most cases the flux direction was opposing, and for pairs in which the flux direction was the same for both sizes, the difference in rates was often too great to provide meaningful results. In addition, variability existed in the measured flux rates between the same size meters over consecutive measurement periods. As a result of scour or burial of seepage meters, only two consecutive 24 hour measurement periods could be made for each seepage meter. Figures 7 through 9 depict the variability in measurements described above for each meter over the six sampling events. The Appendix lists the results of each of the six sampling events.
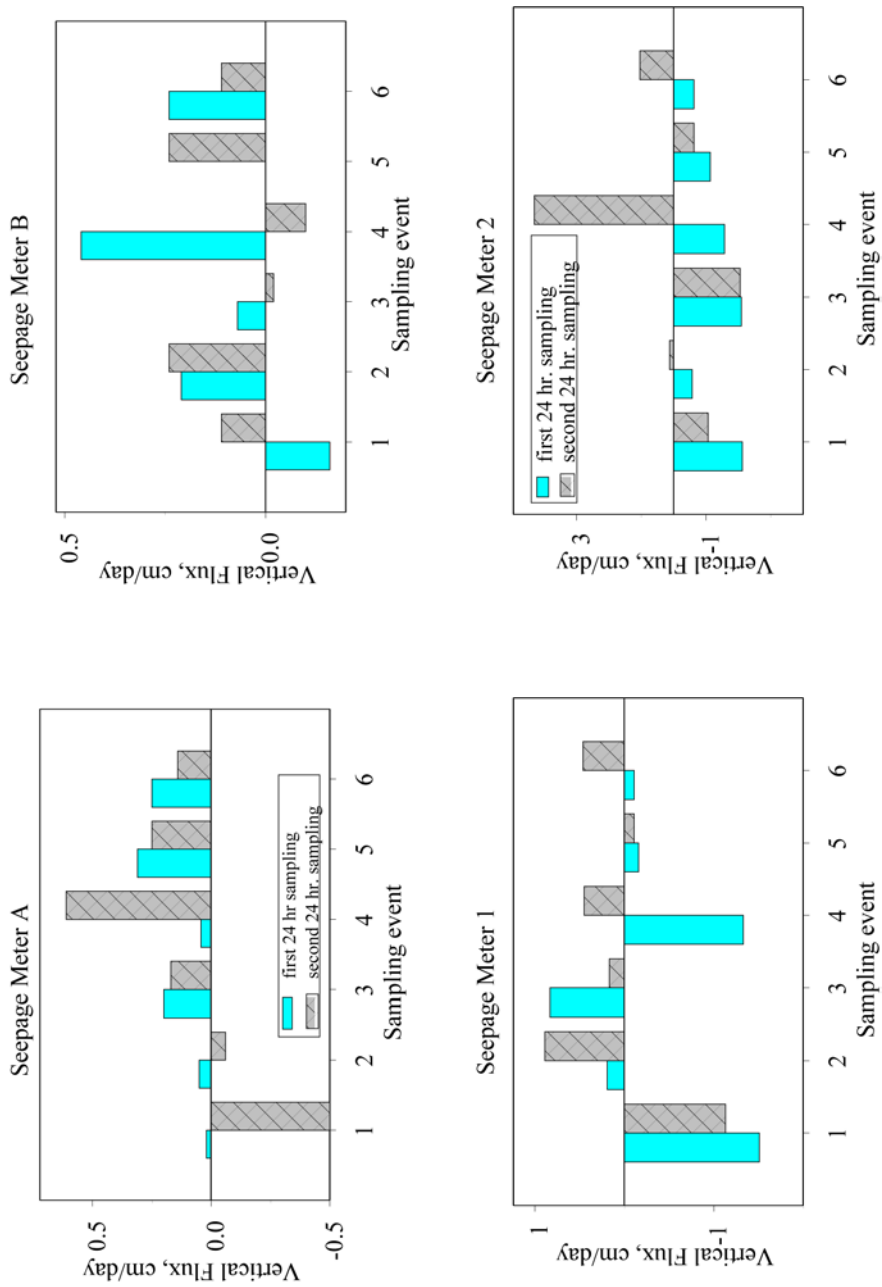
Figure 7. Measured vertical flux rates over consecutive 24 hour measurement periods for seepage meter pairs A-1 and B-2.
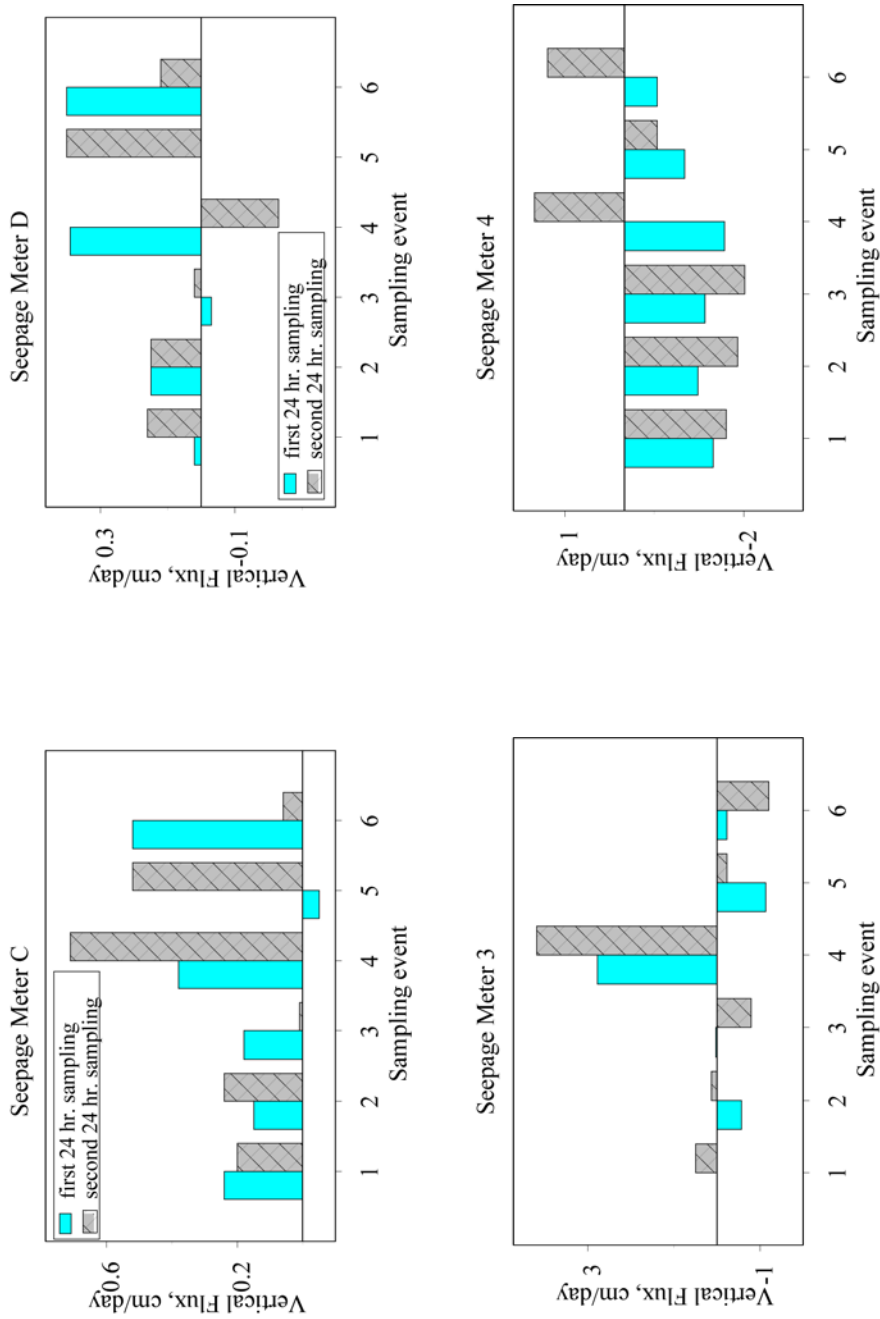
Figure 8. Measured vertical flux rates over consecutive 24 hour measurement periods for seepage meter pairs C-3 and D-4.
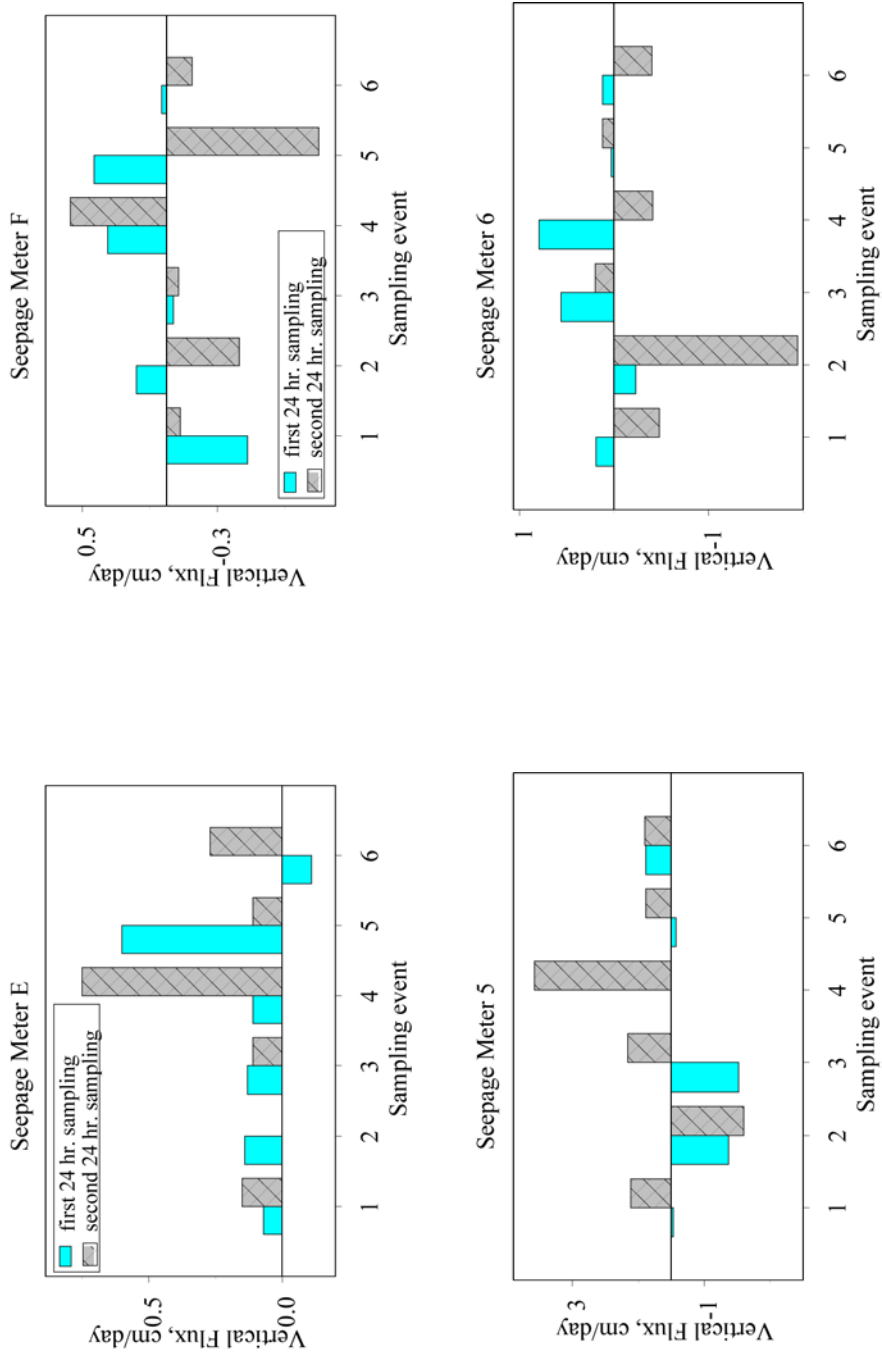
Figure 9. Measured vertical flux rates over consecutive 24 hour measurement periods for seepage meter pairs E-5 and F-5.

The smaller seepage meters (numbered seepage meters in figures 7 through 9) showed greater variability over consecutive measurements than the larger seepage meters, consistent with the findings of Isiorho and Meyer (1999). The results of the January and February 2004 (sampling events 3 and 4) gave inconclusive results for comparisons made between measured rates using shower and medical collection bags and comparing those rates to measured rates using the packaging bags (Appendix). However, repeat measurements made with the shower bag attached to the large seepage meter gave consistent results. During the January 2004 visit, seepage meter B measured rates of 0.21 cm/day and 0.24 cm/day in two repeat measurements and seepage meter C measured the same seepage rate, 0.15 cm/day, over a 48 hour period. The same pattern resulted for seepage meter A during the February 2004 visit which measured a flux rate of 0.20 cm/day and 0.17 cm/day for consecutive measurements. The July and September 2004 site visits (sampling events 5 and 6) used only the thin-walled packaging bags attached to both meters, and inconsistencies in direction and magnitude of measured rates indicated no apparent pattern in seepage rates.

It was unclear if the variability observed between the two types of seepage meters was a result of spatial variability in the hyporheic flow paths at the sediment-water interface, a result of scour and burial problems encountered with the seepage meters, or unexplainable factors affecting the performance of the seepage meter and/or collection bags. In addition, since only 2-3 repeat measurements could be made at each of the field visits before meters were scoured out, the seepage rates of pairs giving similar estimates are difficult to accept. More repeat measurements should be conducted before accepting

the estimates of flux using this method. In addition, measurements over a smaller time span (every 4-6 hours) over a 2-3 day period should also be conducted to determine if evapotransporation is a factor in measured rates. Although the packaging bags performed exceptionally well in the laboratory test tank, their performance in the field was outdone by the shower bag. The very slow seepage rates encountered in the field were not enough to overcome the kinks and folds of the packaging bags and as a result they would only fill to the shape constrained by the respective housing unit. Conversely, the housing unit for the shower bag matched the rectangular shape of the shower bag and did not constrain the collection bag. Overall, the direct measurement technique as applied to this study resulted in inconclusive flux results. The moving streambed bottom seemed to be the limiting factor in applying this simple technique, and overcame any other attempts to limit variability in measurements made. The seepage meters seemed to fail in this relatively high-energy stream with its mobile bed.

Laboratory Measurements

<u>Laboratory Methods</u>

The performance of the three types of collection bags used in this study was tested in a laboratory seepage tank to examine the effects of bag thickness on measured rates of vertical flux. A cylindrical test tank with an inside diameter and height of 152 cm contained a 91 cm thick layer (1.67 m^3) of medium sand placed over a 15 cm layer (0.28 m^3) well-sorted, rounded gravel, with a medium size of 1.9 cm (Figure 10). Vertical flux was generated within the tank by introducing a constant head water source to the bottom of the tank, and flow was measured by an in-line flow meter. A data logger recorded both the flow rate delivered to the bottom of the tank and pressure head measured by a pressure transducer located in the constant head water source tank. The data logger was programmed to control the pump in order to maintain a constant water level. An overflow opening was used to maintain water level within the constant head source tank to within 0.15 cm inside the tank.
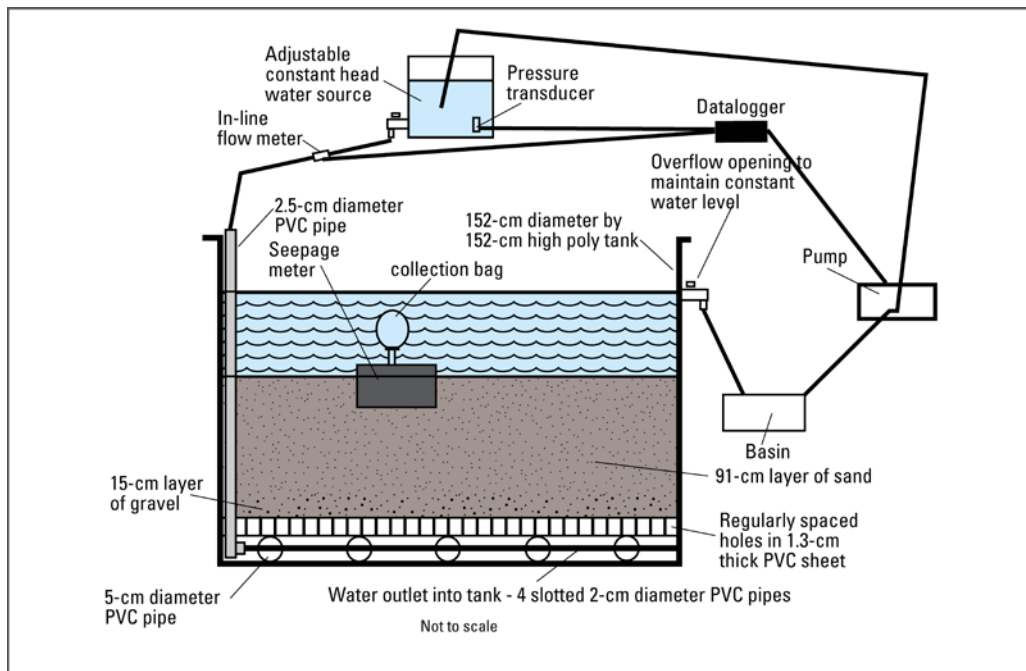
Figure 10. Laboratory test tank set-up used for testing of different types of collection bags attached to seepage meters. (Test tank design and set-up by Michael Menheer, USGS, 2004).

A total of four seepage meters was placed in the test tank: (2) large and (2) small seepage meters. The system was allowed to equilibrate for 24 hours prior to the test runs. The three types of collection bags used were a 1800 ml Sun Shower Solar Bag [®], a 2000 ml medical urine collection bag, and a 2000 ml Void-Fill[®] packaging bag (figure 11). The wall thickness of each of the collection bags was measured with venier calipers at 0.41 mm, 0.26 mm, and 0.04 mm, respectively. The collection bags were pre-filled with a known volume of water and attached to the seepage meters using a 10 cm length of 0.64 cm i.d. vinyl tubing. The seepage meters and connected bags were placed in the test tank for a period of 60 minutes for each test run. Seepage meters of the same cross-sectional area were considered pairs for each test run.

Two separate sets of test runs were conducted. The objective of the first set of test runs (test runs 1 through 8) was to compare the results of measured vertical seepage rates to the known vertical test tank seepage rates. For these tests runs, a packaging bag and a medical bag were connected to the small seepage meters and a packaging bag and shower bag were connected to the large seepage meters. At the end of a test run the collection bags were disconnected, weighed and recorded.

The second set of test runs (test runs 9-12) was conducted using only the packaging bags. The objective of these test runs was to evaluate the ability of the collection bag to fill under various test scenarios. The vertical flux rate in the test tank was set to a known constant positive flux rate for the duration of all test runs conducted. The specifics for each of these test runs are presented in the results section.

Figure 11. Bag types as photographed from left to right: Sun Shower Solar® bag, medical collection bag, and Void-Fill® packaging bag.

Laboratory Results

A relative percent difference (RPD) was used to describe the variability between the measured vertical seepage rates and the known test tank vertical seepage rate for each of the twelve test runs. The RPD was calculated as the difference between the measured and known seepage rates divided by the average of the two values and expressed as a percentage. A RPD of less than 10% between the known and measured seepage rates was considered acceptable for the test runs conducted in the test tank. Table 2 lists the resulting variability for test runs 1-8 in which the performance of the three different bags types was compared to the known test tank vertical flux. The median RPD for the shower bag connected to a large seepage meter was 121%, and the median RPD for the medical bag connected to small seepage meters was 96.5%. The median RPD for the packaging bags connected to the large and small seepage meters was 13.7 and 7.6%, respectively. The results of test runs 1 through 8 are depicted as box plots in figure 12.

Table 2. Results of measured to known vertical seepage rates for collection bag types.

TEST RUN #	Seepage Meter Type	Bag type	Measured Vertical Flux rate, cm/day	Known Test Tank Vertical Flux, cm/day	RPD, %
1	Large	shower Bag	3.45	17.1	133
	Large	packaging bag	NA[1]	17.1	NA[1]
	Small	packaging bag.	18.5	17.1	7.66
	Small	medical bag	11.6	17.1	38.4
2	Large	shower Bag	2.97	16.8	140
	Large	packaging bag	14.6	16.8	13.7
	Small	packaging bag.	16.3	16.8	3.02
	Small	medical bag	5.65	16.8	99.1
3	Large	shower Bag	4.88	19.0	118
	Large	packaging bag	16.4	19.0	14.4
	Small	packaging bag.	17.7	19.0	6.81
	Small	medical bag	5.46	19.0	111
4	Large	shower Bag	3.83	17.1	127
	Large	packaging bag	15.1	17.1	12.8
	Small	packaging bag.	15.7	17.1	8.38
	Small	medical bag	1.56	17.1	167
5	Large	shower Bag	2.57	17.1	148
	Large	packaging bag	14.5	17.1	16.6
	Small	packaging bag.	18.5	17.1	7.46
	Small	medical bag	4.19	17.1	121
6	Large	shower Bag	7.18	17.5	83.6
	Large	packaging bag	18.5	17.5	5.34
	Small	packaging bag.	15.9	17.5	9.54
	Small	medical bag	10.2	17.5	52.6
7	Large	shower Bag	4.02	5.21	35.5
	Large	packaging bag	5.65	5.21	25.7
	Small	packaging bag.	5.69	5.21	8.85
	Small	medical bag	11.2	5.21	72.9
8	Large	shower Bag	2.42	5.58	79.0
	Large	packaging bag	5.06	5.58	9.76
	Small	packaging bag.	6.00	5.58	7.23
	Small	medical bag	1.95	5.58	96.5

[[1] no results due to set-up problem, tubing not properly connected to meter]
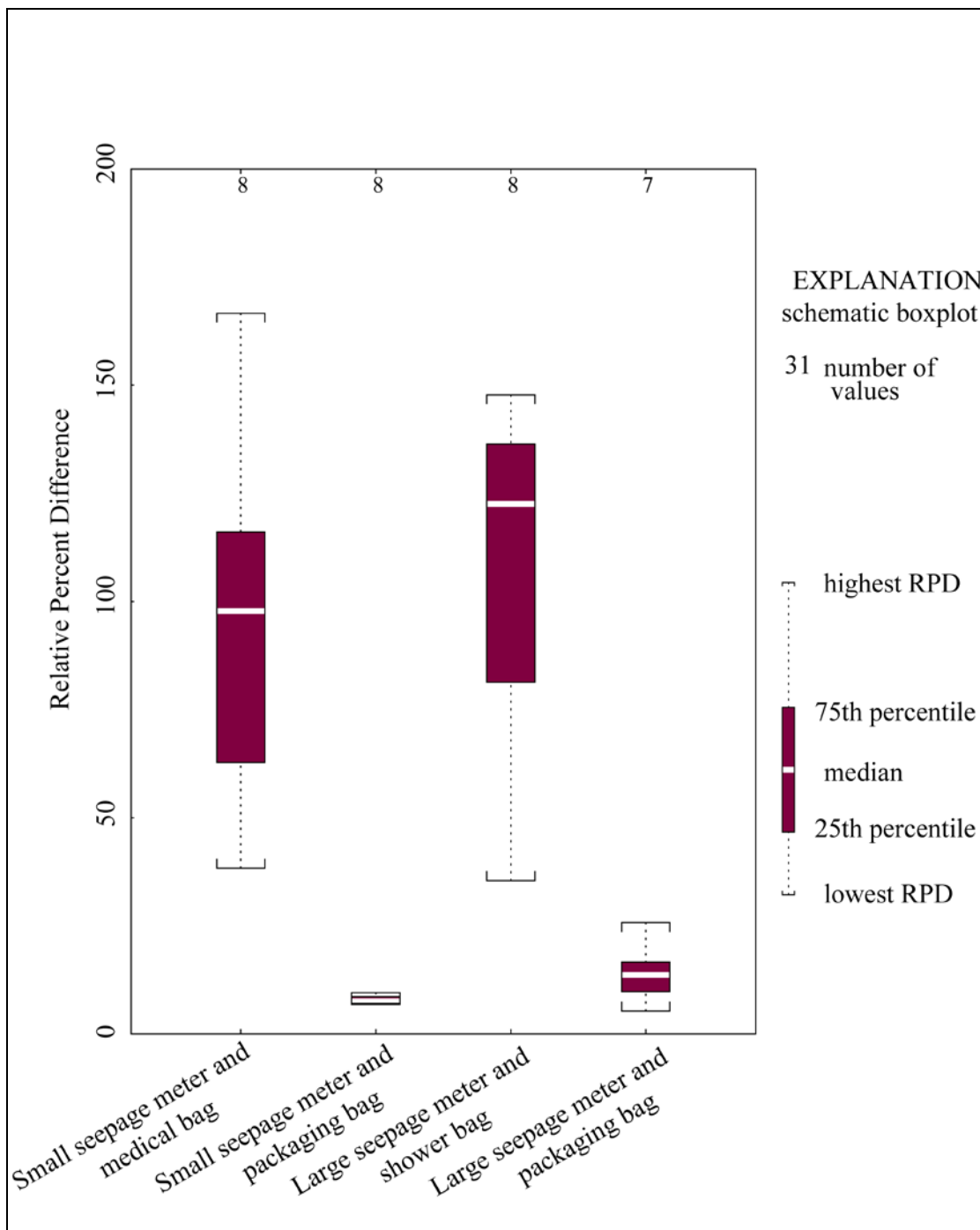
Figure 12. Boxplots of relative percent difference (RPD) between measured and known seepage rates.

The results from test run 1 through 8 indicate that the thin walled packaging bags performed better than the thicker walled collection bags under an applied constant head. The thin walled bags appear to be more compliant than the thicker walled bags and filled easily. The compliance of bags to fill under applied hydraulic head is affected by the size, shape and the membrane thickness of the bag. The hydraulic head required to cause flow into the collection bags is expected to remain relatively constant until the bags fill with enough water to cause stretching, at which point the volumetric flow into the bag will decrease. Furthermore, if the membrane thickness of the collection bag is too large, the volumetric flow into a bag may reach a point where it rapidly decreases or ceases because the hydraulic head is not enough to overcome the resistance of the thicker walled bag. Additional hydraulic head would be necessary to overcome the resistance and continue filling the bag. The high RPD for both the medical bag and shower bag is likely a result of the latter, as the applied constant head during the test runs remained relatively constant throughout each test run and the collection bags never filled to maximum capacity in any of the test runs. The volumetric flow rate that the flow meter measured at the beginning and end of each test run was recorded and a RPD was calculated.

The RPD between the flow rates at the beginning and end of each test run ranged from 0% to 7.6% for all test runs (table 3).

Table 3. Comparison of applied flux rate in test tank at beginning and end of each test run as a percent difference.

Test Run	Tank Flux Rate at start of test, ml/ min (flow-thru meter)	Tank Flux Rate at end of test, ml/ min (flow-thru meter)	RPD
1	219	223	2.2
2	214	209	2.2
3	242	233	3.9
4	219	219	0.3
5	219	204	6.5
6	223	233	4.3
7	66.5	67.2	1.1
8	71.3	71.4	0.1
9	233	233	0.0
10	233	233	0.0
11	61.7	57.0	7.6
12	66.5	68.2	2.6

In test runs 9 through 12 the bag compliance of the thin walled packaging bags was tested under four different test scenarios (table 4). The results of test run 9 indicate that the empty collection bag would fill if the tubing was filled, however the RPD was twice the acceptable median RPD. Test runs 10 and 11 compare the results starting with a partially filled collection bag and attaching the hosing that is filled (test scenario 2) or empty (test scenario 3). In test scenario 3, it was unclear as to whether the applied constant head filled the tubing before flow into the bag occurred, or whether the initial volume that the bag contained filled the tubing to initiate flow into the collection bag. The median RPD for this test scenario was 43.1%. The collection bags under test scenario 2 gave the best results. The results indicate that a small initial volume void of any air bubbles or kinks in the collection bag or tubing resulted in an average RPD between measured and known flux rates of 6.4% and 5.4% for the large and small seepage meters, respectively.

The results of test run 12, in which empty tubing and an empty collection bag were attached to the seepage meters, indicate that, the RPD between the known and measured vertical flux rate was much greater than the acceptable difference. The high RPD (median RPD of 90.3%) for this test scenario appears to be related to the energy required to open a bag that is initially empty. Other investigators (Erickson, 1981; Shaw and Prepas, 1990a, 1990b; Belanger and Montgomery, 1992; and Landon and others, 2001) have reported problems with seepage meter performance when using bags that were initially empty.

Table 4. Results of test runs 9-12

TEST RUN #	Seepage Meter	Bag type	Test Scenario Description	Test Scenario #	Measured Vertical Flux rate, cm/day	Known Test Tank Vertical Flux, cm/day	Percent Difference
9	Large	Packaging Bag	0 initial volume, tubing filled	1	23.00	18.24	26.1
	Large	Packaging Bag	0 initial volume, tubing filled	1	22.53	18.24	23.5
	Small	Packaging Bag	0 initial volume, tubing filled	1	15.22	18.24	16.6
	Small	Packaging Bag	0 initial volume, tubing filled	1	15.09	18.24	17.3
10	Large	Packaging Bag	50 ml initial volume, tubing filled	2	19.49	18.24	6.8
	Large	Packaging Bag	50 ml initial volume, tubing not filled	3	21.40	18.24	17.3
	Small	Packaging Bag	50 ml initial volume, tubing filled	2	16.59	18.24	9.1
	Small	Packaging Bag	50 ml initial volume, tubing not filled	3	11.58	18.24	36.5
11	Large	Packaging Bag	50 ml initial volume, tubing filled	2	4.54	4.83	6.0
	Large	Packaging Bag	50 ml initial volume, tubing not filled	3	7.37	4.83	52.4
	Small	Packaging Bag	50 ml initial volume, tubing not filled	2	4.89	4.83	1.2
	Small	Packaging Bag	50 ml initial volume, tubing filled	3	1.78	4.83	63.3
12	Large	Packaging Bag	0 initial volume, empty tubing	4	13.80	5.21	165
	Large	Packaging Bag	0 initial volume, empty tubing	4	13.91	5.21	167
	Small	Packaging Bag	0 initial volume, empty tubing	4	1.97	5.21	62.1
	Small	Packaging Bag	0 initial volume, empty tubing	4	2.49	5.21	52.2

Overall, the laboratory results of the three bag types tested indicate the thin compliant packaging bags performed better than the medical and shower bag under the applied laboratory conditions. In addition, results of test runs 9-12, (table 4) indicate the packaging bags performed best when starting with an initial volume and filled tubing prior to attachment to seepage meters (test scenario 2). Results of each of the test scenarios described in table 4 are depicted in figure 13.
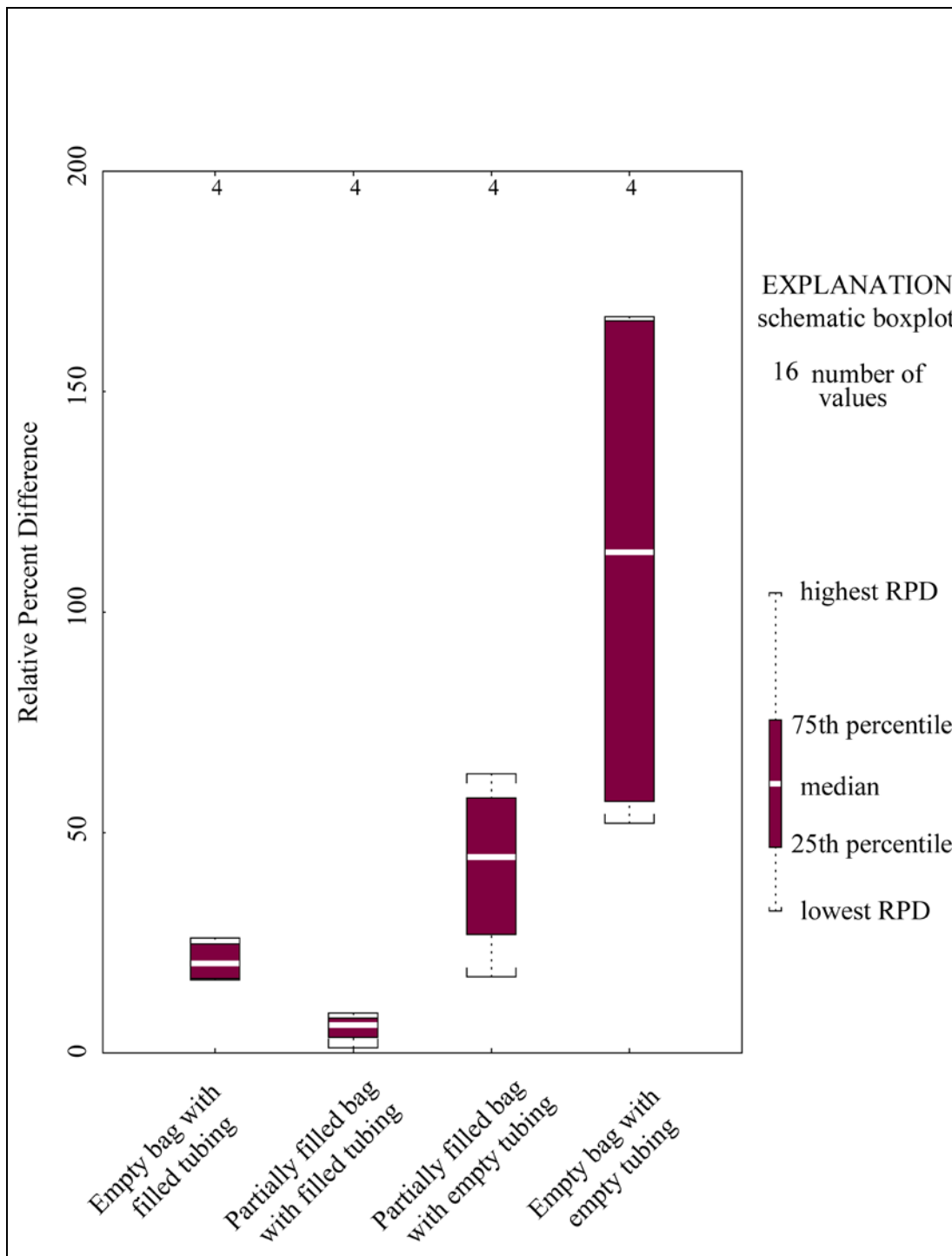
Figure 13. Boxplots of relative percent difference of bag compliance under various test scenarios.

ESTIMATES OF HYDRAULIC CONDUCTIVITY

Hydraulic conductivity (K) represents the ability of a porous medium to transmit water through its interconnected voids. Streambed K plays an important role in the interactions occurring between the surface water and ground water. Streambed K can have lower values than the underlying surficial aquifer because silt, clay and organic materials are often deposited in streams, thereby restricting the surface water/ ground water (sw/gw) fluxes (Larkin and Sharp, 1992; Conrad and Beljin, 1996). Estimates of this parameter are necessary to quantify the magnitude and spatial distribution of sw/gw interactions. Streambed K has been estimated using a variety of approaches including numerical modeling (Yager, 1993; Sophacleous and others, 1995), and analytical solutions for pumping aquifer tests conducted near streams (Hantush, 1965; Hunt, 1999), chemical tracer experiments (Harvey and Bencala, 1993; Hart and others, 1999), coupling heat as a tracer with numerical models (Bravo and others, 2002; Su and others, 2004), physical in-stream methods, and streambed sediment grain size analysis (Hazen, 1911; Shepard, 1989; and Alyamani and Sen, 1993).

Estimates of streambed hydraulic conductivity for this project were estimated by grain size analysis of collected streambed sediments and slug tests. Although slug tests measure K values that depend on horizontal and vertical flow, and K values from grain-size methods are non-directional, the two methods are directly compared for the purpose of characterizing streambed K values.

Review of Literature

In-stream methods for determining K include slug tests (Lee and Cherry, 1978; Duwelius, 1996; Cey and others, 1998; Springer and others, 1999), in situ permeameter tests (McMahon and others, 1995; Duweilius, 1996; Lindgren and Langdon, 2000; Rosenberry, 2000), and seepage flux measurements using seepage meters coupled with measurement of hydraulic gradient through the streambed (Lee and Cherry, 1978; Wolf and others, 1991). The latter method can give variable estimates of K due spatial variation of hydraulic head gradients within a streambed. Kelly and Murdoch (2003) recognized the issue with this method and developed two physical techniques to measure K in streams or lakes. The first technique uses a device called a piezo-seep to estimate vertical hydraulic conductivity (K_v) at relatively shallow depths using a pan similar to a seepage meter with a single monitoring well installed vertically through the pan. The second technique uses a shallow well pumped at a constant rate and a nearby observation well to measure drawdown. The collected field data are coupled with a theoretical solution, and yield estimates of both the horizontal and vertical conductivities, K_h, and K_v. Cardenas and Zlotnik (2003) present a fast, efficient constant-head injection test for in situ method of estimating of K that uses a manually driven monitoring well into the streambed.

A comparison of in-stream methods for measuring the K in sandy streambeds was conducted by Landon and others (2001) and included slug tests, constant-head extraction tests, combination of seepage meters and hydraulic-gradient measurements, falling and

constant-head permeameter tests and grain-size analysis. Their study found that field permeameter tests analyzed using the Darcy equation and coupled seepage meter/hydraulic-gradient measurements were not preferred techniques based upon test design and logistical concerns; seepage meters often fail in relatively high-energy flow streams with mobile beds. However, the Hvorslev analysis of field permeameter tests was the most robust method for determining K in the shallow subsurface. At greater subsurface depths, slug tests or core samples represent more practical in-stream approaches for determining K, especially if deeper streambed deposits have lower permeability that limit the ground water/surface water fluxes. An important conclusion from their study was that the selection of method may matter less than making multiple measurements to adequately characterize the variability across transects. Furthermore, it is important to consider the location of low-permeability sediments when selecting a method of analysis.

Estimates of streambed K can also be obtained from samples collected for grain-size analysis. The K of unconsolidated materials has been related empirically to particle-size distribution by a number of investigators (Hazen, 1911; Krumbein and Monk, 1942; Harleman and others, 1963; Masch and Denny,1966; Wiebenga and others 1970; Shepard, 1989). These studies determined an empirical relationship between K and some statistical parameter (geometric mean, mode, standard deviation, or effective diameter) that often do not fully represent the entire grain-size distribution curve. Consequently, different statistical parameters yield different K values. Alyamani and Sen (1993) propose an alternative methodology for estimating K from grain size distribution curves

by relating K to the initial slope and intercept of the grain-size distribution curve and suggest that this method yields better estimates of K than methods that rely on one or more statistical parameters. Their method places emphasis on the first half of the grain-size distribution curve rather than the large grain diameter domain. The logic in this approach is that the addition of large grain sizes to fine sizes will not alter the K, but that adding fine sizes to large grain sizes will have a very significant effect on the K. Hence, instead of relying on one statistical parameter, their approach uses an effective range of grain-size diameters for calculating a K.

Methods

<u>Grain Size Analysis</u>

A total of six sediment cores were collected from near each of the in-stream monitoring well pairs depicted in figure 14, and a sieve test analysis was conducted on each core. The length of collected cores ranged from 25-46 cm and consisted of a homogeneous medium to coarse grained, well-sorted sand. The weight percent from each sieve size class was used to calculate a cumulative weight percent, and a grain size distribution curve was generated for each core collected. The resulting curves depicted in figure 15 represent the grain size distribution curves for the samples collected at the upstream and downstream transect. These curves were used to approximate the K of the streambed sediments by three grain-size methods: the Hazen approximation, the Shepard approximation, and the Alyamani and Sen approximation.
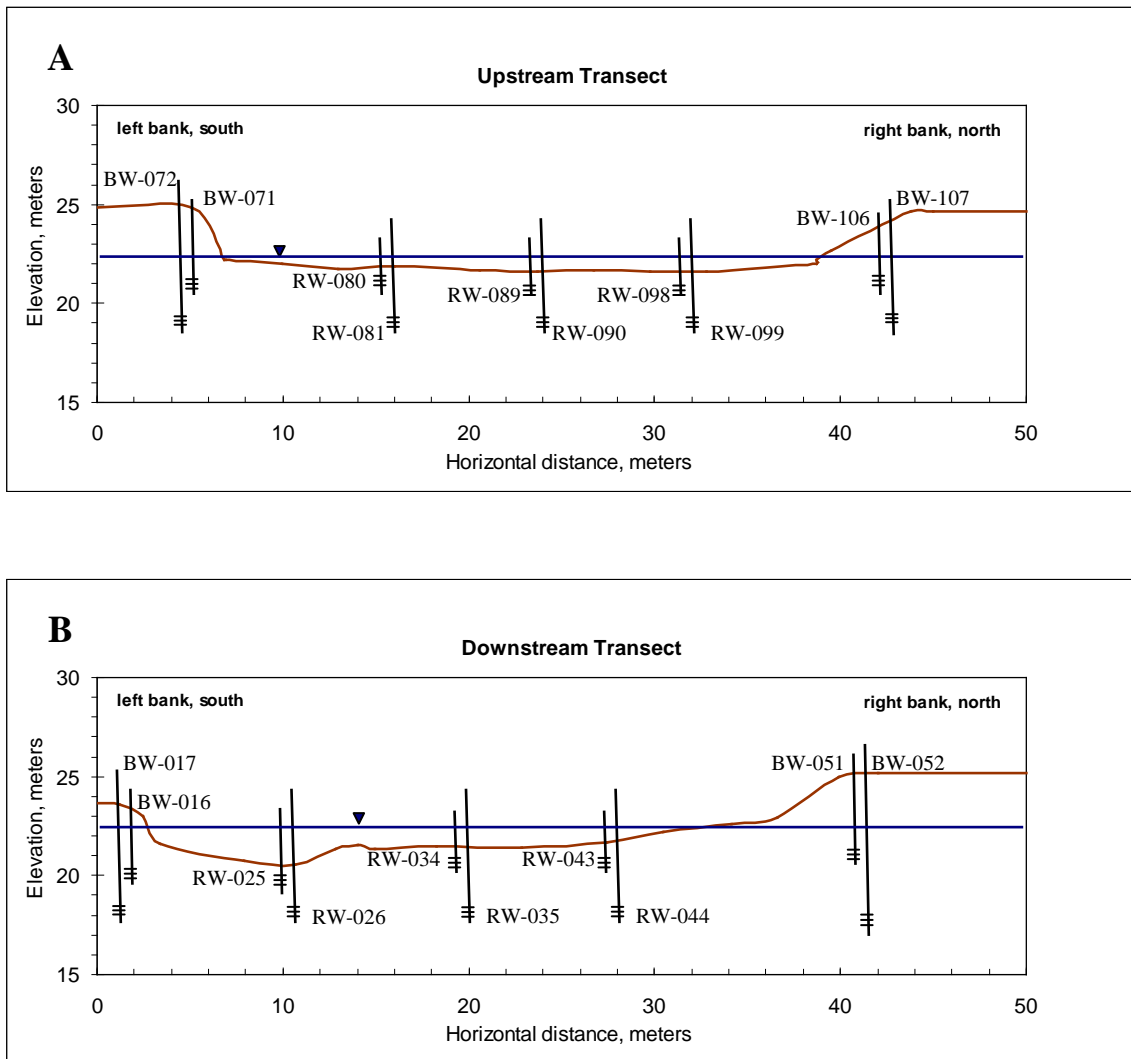
Figure 14. Cross-sectional schematic of monitoring well name and location for the upstream (A) and downstream (B) transects.
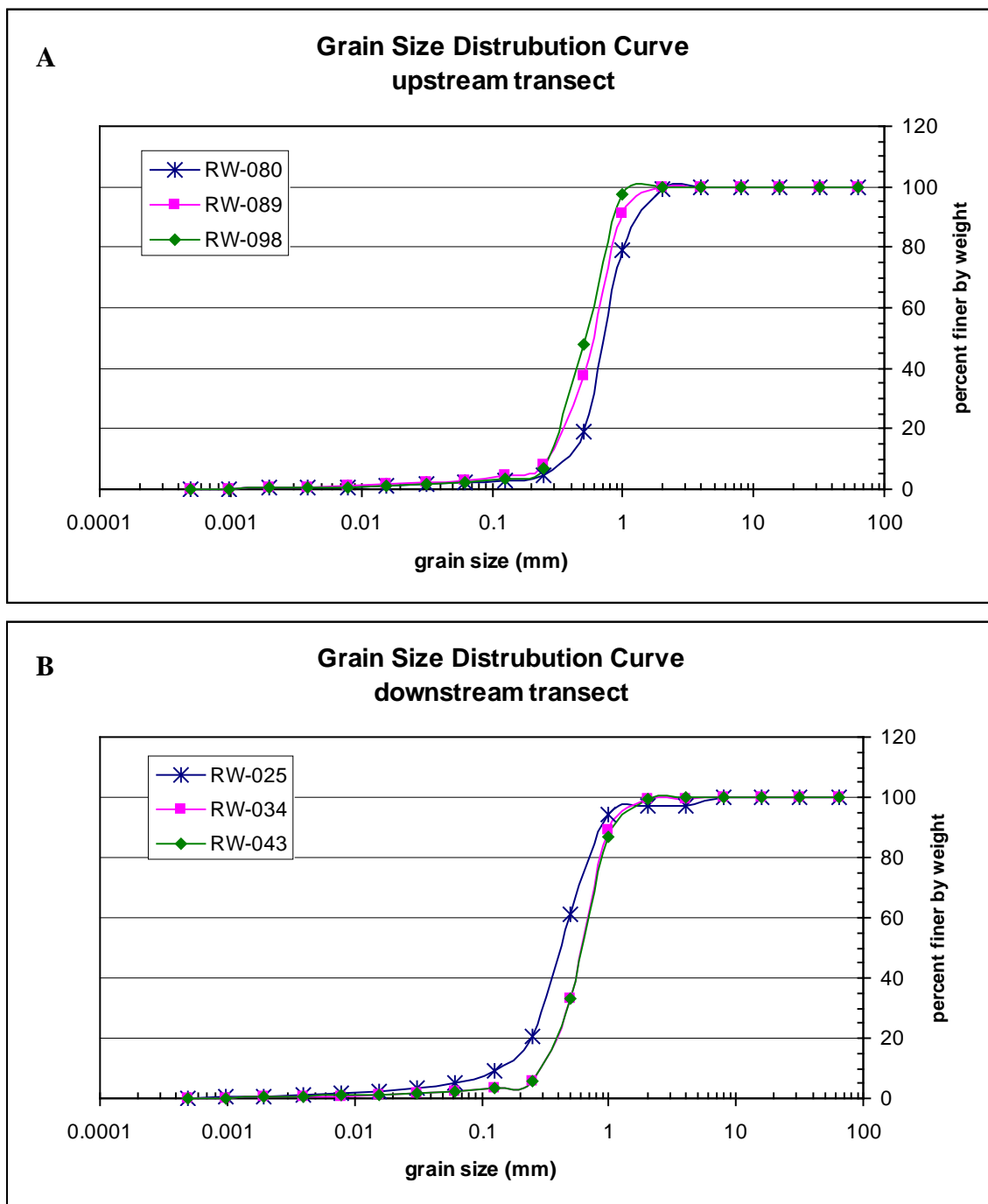
Figure 15. Grain size distribution curve for sediment cores collected at the upstream transect (A) and downstream transect (B).

Hazen Approximation

Grain size distribution curves can be used to estimate the K of sands where the effective grain size is between approximately 0.1 to 3.0 mm (Fetter, 2001) by applying the Hazen method (Hazen, 1911). The effective grain size, d_{10}, is the size corresponding to the 10 percent line on the grain size distribution curve and represents passing of 10% of the sample during the sieve analysis. These values from the generated grain-size distribution curves were applied to the Hazen approximation for K, is as follows:

$$K = C*(d_{10})^2 \qquad \text{[equation 1]}$$

where:

K = hydraulic conductivity (cm/s)

d_{10} = effective grain size (cm)

C = coefficient based on grain size (see Fetter, 2001)

Shepard Approximation

The work of Hazen (1911) demonstrated that K could be related to the square of a characteristic dimension of sediment. Shepard (1989) analyzed data from 18 published studies where K had been related to grain size. He used the data sets to produce an idealized graph that related K to the mean grain diameter, d_{50}, for different sediment types. It is from this graph that both C and j are determined. He found that all studies could be related to the general formula:

$$K = C*(d_{50})^{j} \qquad \text{[equation 2]}$$

where:

C = shape factor

d_{50} = mean grain size (mm)

j = exponent based on textural maturity

Alyamani and Sen Approximation

    This method of estimating K relates the K to the initial slope and intercept of the grain-size distribution. A graphical procedure is applied to the generated grain-size distribution curves (Alyamani and Sen, 1993) and K is calculated from the following equation:

$$K = 1300[I_{o} + 0.025(d_{50} - d_{10})] \qquad \text{[equation 3]}$$

where:

K = hydraulic conductivity (m/day)

I_{o} = intercept at horizontal axis

$d_{50} - d_{10}$ = difference between the effective (d_{10}) and average grain (d_{50}) size

<u>Slug Tests</u>

Slug tests are performed by changing the head in a well that has achieved steady state, and measuring how rapidly the well returns to equilibrium. The K of the material surrounding the well screen will control this recovery rate. Slug test are typically performed by placing a weighed slug (such as a sand filled section of PVC pipe) into a well and measuring the recovery of the well (slug test), or removing a slug from the well after it has achieved equilibrium (bail test) and measuring the recovery of the well. Slug tests were performed on 18 of the 20 monitoring wells located at the study site on September 20th and 21st, 2004. Eight of the slug tests were performed on the riparian bank monitoring wells screened at approximately 3.5 m and 5 m below land surface, and 10 were performed on the in-stream monitoring wells screened at approximately 0.5 m and 3 meters below the sediment/ water interface. Two different slugs were used, both were made of out of PVC plastic tubing, filled with sand, capped and sealed (dimensions: 45.7 cm by 3.2 cm and 91.4 cm by 3.2 cm, or 1.5' by 1.25" and 3' by 1.25"). The larger slug was used in the monitoring wells that were screened at greater depths and the smaller slug was used in the monitoring wells that were screened at shallow depths. Aquistar PT2X $^{®}$ pressure transducers were used to measure and record the head changes during these slug tests. These transducers were hung in place by a cable, and placed at specified distances below the static water level in the well. The transducers were set to record at 0.1 second intervals, and allowed to equilibrate with the well before the slug was dropped or removed.

Slugs were dropped and removed twice without removing the transducer for each monitoring well, and this data set was considered a set of slug tests. Manual water level measurements were taken and recorded before each set of slug tests and using a steel tape. The length of time for each individual slug test ranged from seconds to minutes, and only 1 monitoring well (BW-016) did not fully recover between tests. This well was screened interval in a silty-clay layer.

In order to calculate the quantitative values of K from the slug test data, the Hvorslev (1951) and Bouwer and Rice (1976) methods of slug test interpretation for unconfined aquifers were utilized in the software package AQTESOLV. Analysis involves matching a straight-line solution to water-level displacement data collected during the slug test. Several assumptions about the aquifer and monitoring wells conditions were made in order to complete the analysis:

1. The aquifer had infinite areal extent.

2. The aquifer is homogeneous and of uniform thickness.

3. The aquifer potentiometric surface is initially horizontal.

4. The aquifer is unconfined.

5. The screened interval of the saturated unit surrounding each monitoring well was assumed to be isotropic.

6. Use of Bouwer-Rice method was assumed appropriate even though this method was developed for rising head, not falling head. Since this method does not include changes in transmissivity in either case, use of the method for falling head (slug removal) was considered acceptable.

Results

Calculated values of K were compared between the applied grain size analysis methods and slug tests performed in the shallow monitoring wells. Sediment core samples used to determine K were approximately 25-46 cm in length and therefore could only be compared to slug tests performed in the shallow in-stream monitoring wells screened at approximately 0.5 meters below the sediment water interface. Sediment core samples were not collected near the bank monitoring wells; therefore no comparisons are made between grain size analysis methods and slug tests performed in the bank monitoring wells.

Hvorslev (1951) and Bouwer and Rice (1976) applications were used from the AQTESOLV software program, to estimate K from slug tests. The collected water-level displacement data for each set of slugs tests input into the program only included the data beginning with the maximum displacement of water level and assigned time zero. The length of the monitoring wells in which the slug tests were performed were more than 8 times the radius of the well and correlate with the form factor presented in Fetter (2001) for the Hvorslev (1951) solution to K in unconfined aquifers. The form factor that AQTESOLV applies to the Hvorslev (1951) and Bouwer and Rice (1976) solutions for unconfined aquifer assumes the form factors as described in Fetter (2001) and Freeze and Cherry (1976), respectively.

An arithmetic mean was calculated from slug tests and grain size analysis for each of the monitoring wells. Tables 5 and 6 present the results of these calculations for the upstream and downstream transects, respectively. The expected K for a medium to coarse sand is approximately 10-1000 m/day (Davis and Dewiest, 1966; Todd, 1980; Freeze and Cherry, 1979; Fetter, 2001). Results from grain size analysis and estimates of K fall within the suggested range and show close agreement between methods (except for RW-043) for monitoring wells. The greatest difference between methods was 87 % (RW-043) and the least was 17% (RW-034 and RW-089). In general, grain size estimates produced K values similar to slug test results.

With the exception of BW-016, the streambed K calculated by the Hvorslev solution was greater than the Bouwer and Rice solution for all slug tests performed. The difference was between 20 to 32 percent at the upstream transect and 20 to 40 percent at the downstream transect. RW-090 and RW-098 had the highest calculated K with an average streambed K of 160 to 215 m/day, respectively. Pebbles and cobbles ranging in size from 2-6 cm were encountered during the installation of the in-stream monitoring wells at this location and the screened interval may be in this pebble/cobble layer. Although the resulting K from the Hvorslev solution was generally higher, it was still within the same order of magnitude and the calculated values are within expected values for a medium to coarse sand.

Table 5. Estimated streambed hydraulic conductivity by various methods at upstream transect

Monitoring Well	Location and type	Grain Size (G) or Slug Test (S)	Method	K (m/day)	Arithmetic Mean (m/day)
BW-107	Bank monitoring well north bank, deep	S S	Bouwer and Rice Hvorslev	70 100	85
BW-106	Bank monitoring well north bank, shallow	S S	Bouwer and Rice Hvorslev	80 120	100
RW-099	River monitoring well river right, deep	-- --	no slug test no slug test	-- --	NA
RW-098	River monitoring well river right, shallow	S S G G G	Bouwer and Rice Hvorslev Hazen Shepard Alyamani and Sen	130 190 110 80 100	120
RW-090	River monitoring well middle, deep	S S	Bouwer and Rice Hvorslev	180 250	220
RW-089	River monitoring well middle, shallow	S S G G G	Bouwer and Rice Hvorslev Hazen Shepard Alyamani and Sen	60 90 50 60 50	60
RW-081	River monitoring well river left, deep	S S	Bouwer and Rice Hvorslev	60 90	75
RW-080	River monitoring well river left, shallow	S S G G G	Bouwer and Rice Hvorslev Hazen Shepard Alyamani and Sen	60 90 50 50 50	60
BW-072	Bank monitoring well south bank, deep	S S	Bouwer and Rice Hvorslev	40 50	45
BW-071	Bank monitoring well south bank, shallow	S S	Bouwer and Rice Hvorslev	50 70	60

57

Table 6. Estimated streambed hydraulic conductivity by various methods at downstream transect.

Monitoring Well	Location and type	Grain Size (G) or Slug Test (S)	Method	K (m/day)	Arithmetic mean (m/day)
BW-052	Bank monitoring well north bank, deep	S S	Bouwer and Rice Hvorslev	70 100	85
BW-051	Bank monitoring well north bank, shallow	S S	Bouwer and Rice Hvorslev	120 170	150
RW-044	River monitoring well river right, deep	S S	Bouwer and Rice Hvorslev	50 70	60
RW-043	River monitoring well river right, shallow	S S G G G	Bouwer and Rice Hvorslev Hazen Shepard Alyamani and Sen	100 160 20 30 90	80
RW-035	River monitoring well middle, deep	S S	Bouwer and Rice Hvorslev	20 20	20
RW-034	River monitoring well middle, shallow	S S G G G	Bouwer and Rice Hvorslev Hazen Shepard Alyamani and Sen	30 50 70 60 70	60
RW-026	River monitoring well river left, deep	S S	Bouwer and Rice Hvorslev	40 60	50
RW-025	River monitoring well river left, shallow	S S G G G	Bouwer and Rice Hvorslev Hazen Shepard Alyamani and Sen	no slug test no slug test 70 60 60	60
BW-017	Bank monitoring well south bank, deep	S S	Bouwer and Rice Hvorslev	80 100	90
BW-016	Bank monitoring well south bank, shallow	S S	Bouwer and Rice Hvorslev	20 20	20

ESTIMATING VERTICAL FLUX USING HEAT AS A TRACER

Temperature is a controlling variable for a stream's aquatic life, both in the water column and in the benthic habitat (streambed sediments). Exchanges that occur between streams and ground-water systems play a key role in controlling temperatures not only in the stream, but also in the underlying sediments. Whenever a difference in temperature exists between two points in a flow path, heat will flow between them by transport in the flowing water (advective heat flow) and thermal conduction through the non-moving solids and fluids (conductive heat flow). Heat as a tracer is a simple yet powerful tool for detecting water movement across the surface water/ ground water (SW/GW) interface when this movement is traced by continuous monitoring of temperature patterns in the streambed and subsurface water.

The use of heat as a hydrologic tracer has several distinct advantages over applied chemical tracers. The temperature signal arrives naturally. The primary measurement is temperature, which is a robust and relatively inexpensive parameter to measure. In contrast to chemical tracers, which often require laboratory analysis before interpretation, temperature data are immediately available for inspection and interpretation (Stonestrom and Constantz, 2003). As a result, analyses of subsurface temperature patterns provide information about surface-water/ground-water interactions.

Streams exhibit diurnal temperature fluctuations due to solar-driven temperature fluctuations at the land surface, whereas ground water is buffered from these temperature

fluctuations at depth. The difference in temperature between streams and ground water provides a means for tracing exchanges between the two systems. In a gaining reach of a river, water is moving upward into the streambed and carries with it the relatively static temperature signal of the ground water. As a result, the temperatures in and beneath the gaining reach are muted compared to the diurnal fluctuations in the stream. Conversely, if the stream is losing and water is moving downward into the streambed, the diurnal temperature signal of the river is carried by advection and conduction into the surrounding sediments. Subsurface temperature patterns at depth will exhibit the diurnal fluctuations seen in the stream. Figure 16 depicts these concepts.
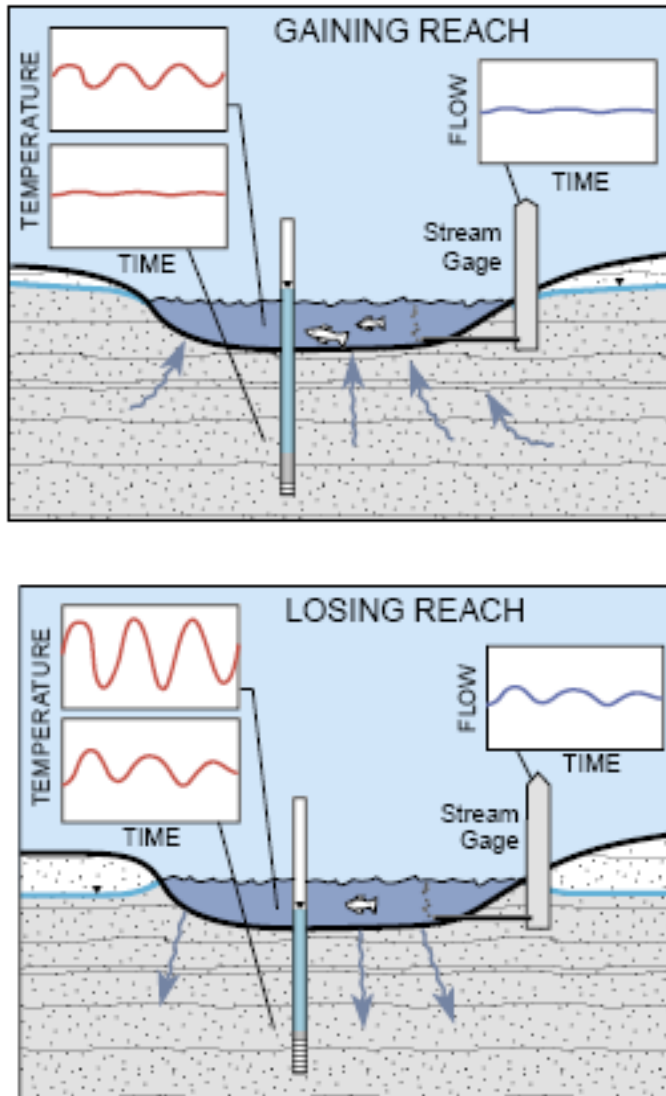
Figure 16. Streamflow and temperature histories for gaining and losing reaches of a stream coupled to the local ground-water system. Ground water is buffered from temperature fluctuations at the land surface. Temperature fluctuations in and beneath the gaining reach are therefore muted (top panel) compared to temperatures in and beneath the losing reach (bottom panel). (Modified from Stonestrom and Constantz, 2004)

Review of Literature

Heat has been used as a tracer of subsurface water movement for more than 40 years. Analytical solutions to equations that govern the coupled movement of water and heat have been derived and applied to estimate the rate at which water travels from the surface to great depths (Rorabough, 1954; Stallman, 1963). Temperature patterns have also been used to study subsurface flow systems ranging from irrigation water in rice paddies to geothermal water beneath volcanoes (Suzuki, 1960; Sorey, 1971). Lapham (1989) used annual temperature records from deep observation wells to identify rates of vertical water flux in several streams in Massachusetts and New Jersey, based on analytical solutions reported in earlier work (Lapham, 1988). However, these analytical solutions were derived for a few idealized cases and resulted in theoretical rather than practical applications due to measurement and computational limitations. Recently, the measurement and modeling of heat and water transport have benefited from significant improvements. Recent innovations in sensor and data-acquisition technology, along with substantial improvements in numerical modeling, present new opportunities for using heat as a tracer of stream-ground water exchanges (Stonestrom and Constantz, 2004). Inexpensive and accurate devices are now available for measuring temperature, water level, and water content. These devices, in conjunction with currently available numerical models, provide general solutions of equations for the coupled transport of heat and water.

Using heat as a tracer, in conjunction with water level measurements can estimate sw/gw exchanges (Silliman and Booth, 1993; Silliman and others, 1995; Stonestrom and

Constantz, 2003; Anderson, 2005). Temperature has been used as a tracer to identify

vertical flux across the SW/GW interface at various locations in the United States. In the

Rio Grande near Albuquerque, New Mexico, Bartolino and Niswonger (1999) used the

USGS numerical model (VS2DH) to match simulated temperature data to observed

temperature, yielding predicted estimates of deep streambed fluxes and spatially-

averaged hydraulic conductivities. Application of heat as a tracer has been used to

examine interactions in alpine streams between stream temperature, streamflow, and

ground water exchanges (Constantz, 1998). The analysis of temperature profiles in

ephemeral stream environments has been used to examine percolation characteristics

beneath arroyos in the Middle Rio Grande Basin, New Mexico (Constantz and Thomas,

1997), to determine streamflow frequency and duration (Constantz and others, 2001), and

to investigate stream losses beneath ephemeral channels (Constantz and others, 2002).

Stonestrom and Constantz (2003) provide technical details of the use of heat as an

environmental tracer as well as a compilation of seven detailed case studies that use

temperature patterns and their interpretation as a hydrologic tool for the assessment of

interactions between surface water and ground water in a variety of environmental setting

throughout the western United States.

Sampling Design and Methodology

A total of 20, 5 cm (2") PVC screened monitoring wells were installed in two

transects across the Merced River. The transects were separated by a distance of

approximately 100 meters. Each transect was equipped with five pairs of monitoring

wells: three pairs in the river and a pair on the right and left bank in the riparian zone.

The monitoring wells were equipped with high-precision temperature loggers and

pressure transducers. Temperature loggers monitored temperature continuously in both

the surface water (above sediment/ water interface) and at three depths within the

streambed at both transects. Pressure transducers located in the stream and below the

streambed collected water-level data that were used to define boundary conditions.

Temperature and pressure head data were input into a USGS numerical model, Variably

Saturated 2-Dimensional Heat (VS2DH), (Healy and Ronan, 1996), and its graphical

interface VS2DI (Hsieh and others, 2000). This program uses an energy transport

approach via the advection-dispersion equation to simulate heat and flow transport.

Estimates of streambed hydraulic and thermal conductivity were input into the model

until model simulations "fit" observed streambed temperatures at depth. This inverse

modeling method uses a visual best fit, and is most sensitive to variations in the input

parameter K.

The pairs of monitoring wells at each transect consist of a shallow and a deep

monitoring well screened at approximately 0.5 meters and 3 meters below the streambed

for the in-stream monitoring wells, and at approximately 3.5 and 5.0 meters below the top

of well casing for the riparian zone monitoring wells. Figure 17 depicts a cross-sectional

view of an equipped transect.
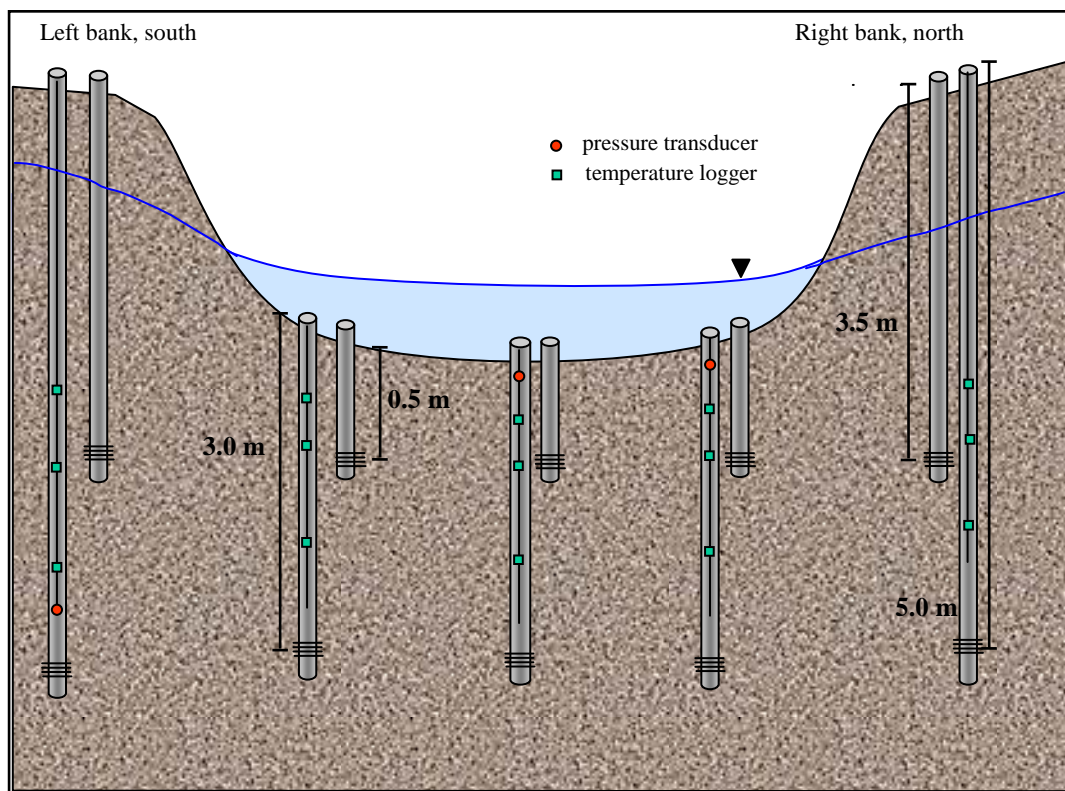
Figure 17. Cross-sectional view of an instrumented transect (not to scale)

The monitoring wells were installed by pumping the streambed sediment out while pushing in a 15 cm (6") PVC casing downward to the desired depth. After reaching the desired depth, the smaller 5 cm (2") PVC monitoring well was inserted inside the 15 cm PVC casing and the 15 cm casing was pulled out of the streambed, allowing the surrounding streambed sediments to collapse around the 5 cm PVC monitoring well. The streambed monitoring wells were installed so that the top of the casing of each of the wells was slightly above the streambed. Once in place, the monitoring wells were sealed with standard pressurized monitoring well caps to prevent stream water from entering the monitoring wells. The same installation procedure was used for the riparian zone monitoring wells; however, a combination of hand augering and pumping was used to install the outer casing to the desired depth. A Monterey sand pack was placed around the screened interval of each of the riparian zone monitoring wells. The wells were then sealed with a bentonite cap and backfilled to land surface.

A string of three HOBO Water Temp Pro temperature loggers was fastened to a small diameter rope, at depths of approximately 0.5, 1.0, and 2.0 meters from the monitoring well cap. The temperature loggers were then weighted with a stainless steel bolt and placed in each of the deep in-stream monitoring wells. The same procedure was used for the riparian zone monitoring wells, however, the temperature loggers were placed at approximately 3.5, 4.0, and 5.0 meters below the top of the monitoring well casing. A temperature logger was also placed in the stream to record stream temperature. A total of 10 pressure transducers was used to record water levels: 8 in four pairs of the

in-stream monitoring wells, 1 in the deep riparian monitoring well at the downstream

transect, and 1 in the Merced River.

The temperature loggers and pressure transducers were set to record temperature and

water level at 15-minute intervals through the duration of the study. Manual water level

measurements were also taken through the study in the riparian zone monitoring wells,

and during data downloads for the in-stream monitoring wells. Because the top of the

casing for the in-stream monitoring wells was underwater (approximately 5-10 cm above

the streambed), a 1.8 meter riser was attached to the in-stream monitoring well and

allowed to equilibrate prior to water level measurements. Figure 14 and table 7 identify

the wells by name, location, and the type of continuous data (temperature and/or pressure

head) recorded in each of the monitoring wells.

Table 7. Monitoring well name, depth, location, and type of data collected

Monitoring Well ID	Screened depth (meters)	Transect	Continuous Data Collected
BW-106	3.5	upstream	none
BW-107	5	upstream	temperature
RW-098	0.5	upstream	pressure head
RW-099	3	upstream	temperature and pressure head
RW-090	0.5	upstream	pressure head
RW-089	3	upstream	temperature and pressure head
RW-080	0.5	upstream	none
RW-081	3	upstream	temperature
BW-071	3.5	upstream	none
BW-072	5	upstream	temperature
BW-051	3.5	downstream	none
BW-052	5	downstream	temperature
RW-043	0.5	downstream	Pressure head
RW-044	3	downstream	temperature and pressure head
RW-034	0.5	downstream	pressure head
RW-035	3	downstream	temperature and pressure head
RW-025	0.5	downstream	none
RW-026	3	downstream	temperature
BW-016	3.5	downstream	none
BW-017	5	downstream	temperature and pressure head

[BW indicates a bank well located in the riparian zone and RW indicates a in-stream monitoring well]

Results

In this study, the application of temperature as a tracer utilized continuous monitoring of water levels, subsurface temperature, as well as the elevation and temperature of the stream. Data were input into the numerical model VS2DH, and estimates of hydraulic and thermal conductivity were input into the model until "best fit" simulations matched observed subsurface stream temperatures. This method requires high precision in the water level data and certainty in the elevations (depths) at which the pressure transducers are placed at. However, due to problems associated with the instrumentation used to record continuous water level elevation, prolonged unexpected high streamflow events and the resulting scour and burial of the monitoring wells; the results of the recorded total head distributions and temperature profiles are discussed prior to the modeling results, as these results affect the final model results.

Total Head Distributions

Total hydraulic head (meters) is defined as the recorded pressure head plus the known elevation at which each of the pressure transducers was placed. A pressure transducer was placed in the river to record continuous stream elevation data. These recorded stream elevations were to be used to calculate differences in total head between the ground water and the river, thereby indicating the direction of flow across the sediment/water interface at the instrumented site. Gaining and losing reaches would be defined from the perspective of the river. A positive value would infer a gaining reach and a negative value would infer a losing reach. However the pressure transducer placed

in the river did not provide the quality of data that the instrument was intended to record for several reasons. Initial study design planned for differences in head between the river and ground water on a very small scale (1-3 cm). Unfortunately, the inherent error associated with the estimated elevation of the location of the pressure transducer placed in the Merced River was greater than the measured head differences between the surface water and ground water. This problem was further complicated with each download of data; when the pressure transducer was removed and downloaded, it was nearly impossible to replace the instrument at an exact height in the well. In addition, the PVC casing that housed the pressure transducer was at approximately a 40° angle from horizontal, and was difficult to replace the instrument at its intended location because it was not free-hanging under gravity.

Pressure transducers located below the streambed in the paired monitoring wells screened below the streambed did not have these limitations. These pressure transducers were attached to the cap of the monitoring wells and allowed to hang freely within the monitoring well. Manual water level measurements taken immediately after data downloads agreed well with recorded water levels to within <0.3 cm. As a result, the paired in-stream monitoring wells (MW) (delta H= deep MW- shallow MW) were used to calculate head differences.

Although the pressure head recorded in each of the streambed monitoring wells agreed with manual measurements, the minor discrepancy between the recorded water level and measured water level seemed to increase in the latter part of the study, suggesting drift in the pressure transducers. The pressure transducers used in this study

were not vented to the atmosphere, and were placed in monitoring wells that were sealed

at the streambed. This type of pressure transducer compensates for atmospheric pressure

by utilizing an additional pressure transducer that records barometric pressure (baro-

logger). The data collected from the baro-logger were subtracted from the recorded head

data collected in the monitoring wells. The atmospheric pressure and water levels

calculated by the baro-logger and the pressure transducers are temperature compensated,

and large changes in temperature over a short period of time can affect how the

instruments calculates water pressure (Davies, 2002).

Figure 18 depicts streamflow and recorded head differences (delta H) between the

deep and shallow monitoring wells at the downstream transect. Collected head data at

the upstream transect is not presented due to vandalism (RW-098 and RW-099) and scour

(RW-089 and RW-090). Data loss occurred for the north in-stream monitoring well pair

(RW-044 and RW-043) between September 2004 and January 2005 (figure 18a).
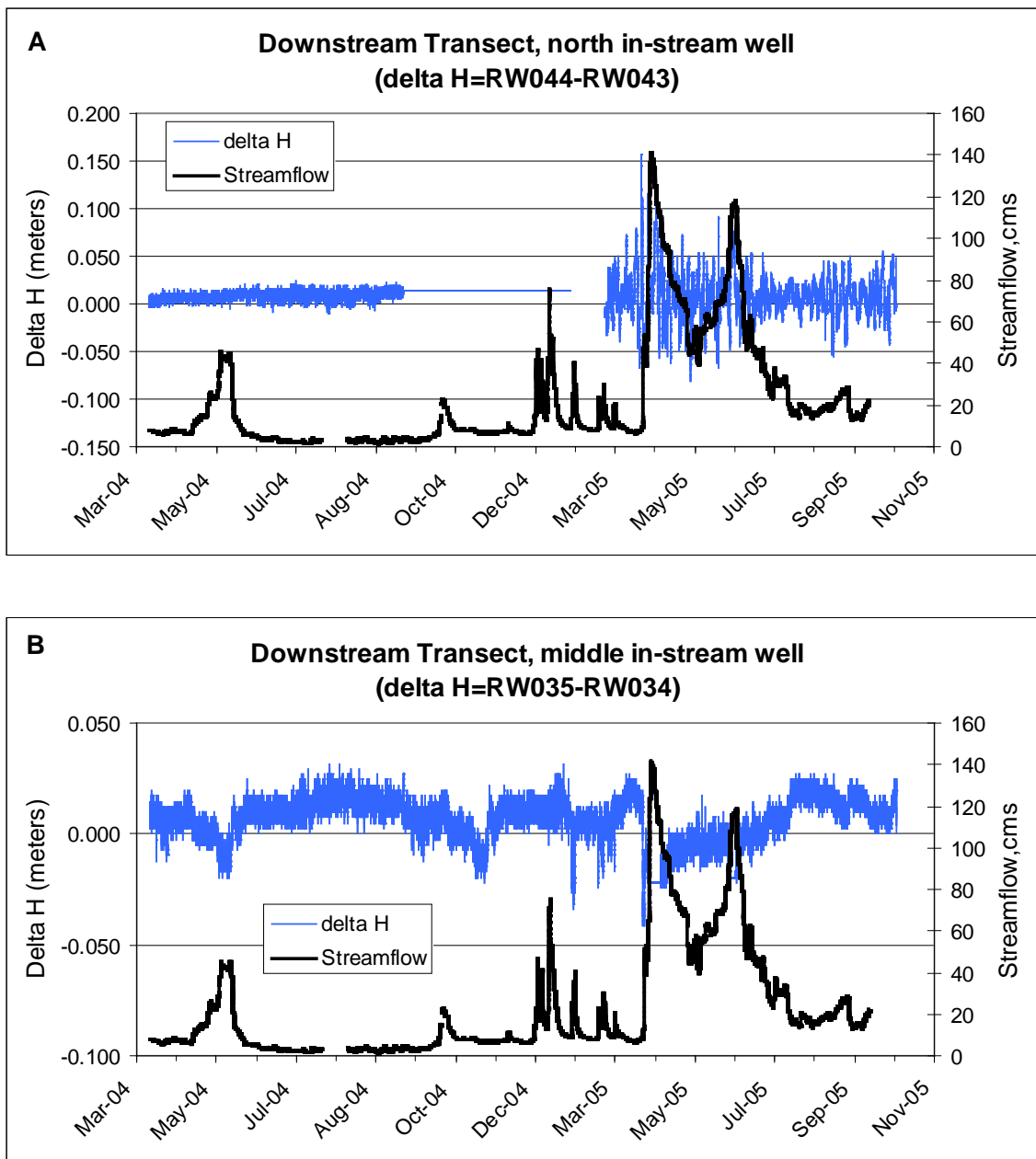
Figure 18. Calculated head differences between deep and shallow monitoring wells and streamflow (**A)** north in-stream wells (**B**) middle in-stream wells.

Delta H values for the middle in-stream monitoring well pair record a generally gaining river throughout the study period with distinct flow reversals (gaining to losing) during high stream flow events. These flow reversals correspond to storm events during winter months, relatively large releases at the Exchequer Dam from mid-April to mid-May, and smaller releases made October as part of the Vernalis Adaptive Management Program (VAMP). The objective of these releases is to help move salmon smolt out to the Sacramento-San Joaquin Delta in April and May and attract spawning salmon to the tributaries in October. The north in-stream monitoring well (figure 18a) recorded large variations in head differences beginning 2005. This was not the case for the middle in-stream monitoring well pair (figure 18b). The water level data collected from the north in-stream well (figure 18 a), did not record flow reversals for the high stream flow events occurring in 2004, and due to the uncertainty of head data recorded during 2005, it is difficult to discern distinct patterns of losing and gaining.

Irrigation season for the study area generally begins in mid-March and ends in September and results in loading of the surficial aquifer. The rise in water levels of the surrounding aquifer is reflected in the water levels of the middle in-stream monitoring well pair, indicating a gaining stream during irrigation season 2004. Irrigation season 2005 did not result in gaining conditions due to large streamflow releases from Exchequer Dam beginning March 2005 and continuing through the end of the study period. These releases were made as a result of spring melt of an exceptionally high snow-pack in the upper part of the basin.

Temperature Profiles

Temperature profiles from the collected temperature data at the upstream and downstream transects are depicted in figures and 19 and 20, respectively. Due to vandalism at the upstream transect, periods of missing data exist for the in-stream monitoring wells (RW-099 and RW-081). RW-090, the middle in-stream well, collected the most complete record, however scouring of this monitoring well is recorded throughout the temperature history and was observed in the field. The temperature recorded at the 0.5 meters below the streambed is nearly the same temperature recorded in the stream or slightly less for most of the recorded temperature history.

During the winter months the stream temperature becomes much cooler than recorded subsurface temperatures, and conversely during the summer months the stream temperature becomes much warmer. At the downstream transect, the in-stream monitoring wells recorded nearly the same temperature patterns at 0.5, 1.0, and 2.0 meters below the streambed. Periods of gaining or losing are recorded, and in general, the subsurface temperatures indicate a slightly gaining to neutral reach throughout 2004, with the exception of mid-April to mid-May 2004 during the VAMP flow events when the temperatures record a losing scenario.
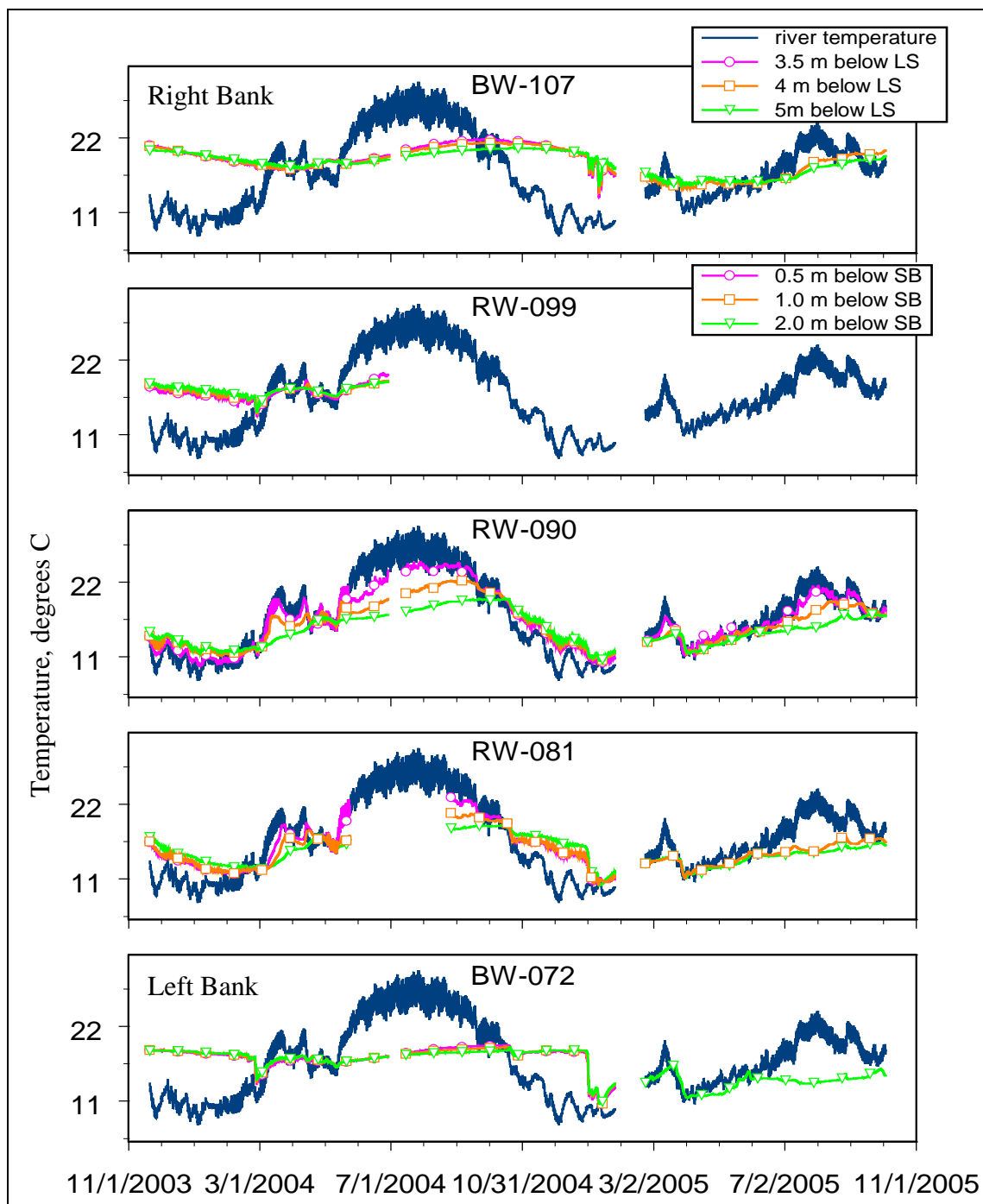
Figure 19. Temperature profiles collected at the upstream transect.
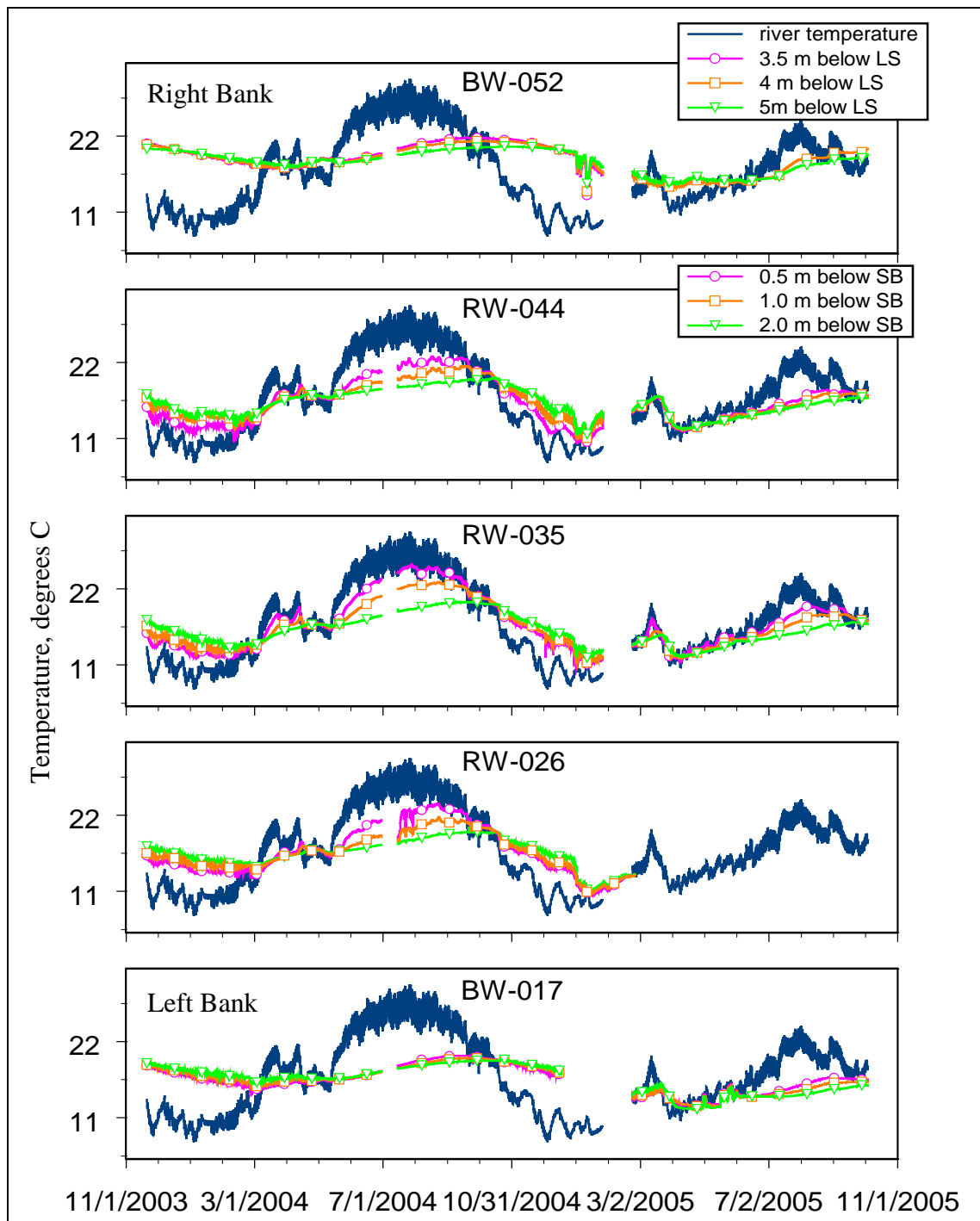
Figure 20. Temperature profiles collected at the downstream transect.

Temperature records from 2005 coincide with the exceptionally high streamflow. This likely caused scour around monitoring wells on the rising limb of the hydrograph and subsequent burial on the falling limb. Field observations support this assumption. As a result, the recorded temperature varied from the intended depths (0.5 m, 1.0 m and 2.0 m, respectively). Despite this concern, the collected temperature data for this time period indicates a losing scenario until June 2005, after which a strongly gaining time period is recorded.

The bank wells for both the upstream and downstream monitoring wells follow the same temperature patterns as the in-stream wells, but to a much lesser extent. The bank wells do not record diurnal temperature variations, but do record slight seasonal changes in summer and winter. However, during the 2005 study period the stream elevation approached or overtook the bank wells on the left bank during the high flow events. As a result, the bank wells BW-017 and BW-072 were sometimes in direct contact with the river and recorded stream temperature.

Flux Estimates from Heat and Water Flow Model Analysis

One-dimensional, cross-sectional modeling of heat and water flow was used to interpret temperature and head observations and to estimate vertical SW/GW fluxes at the downstream transect. Vertical one-dimensional models with 2-cm grid-blocks was calibrated for each of the deep monitoring wells at the downstream transect and each well was modeled separately (figure 21).
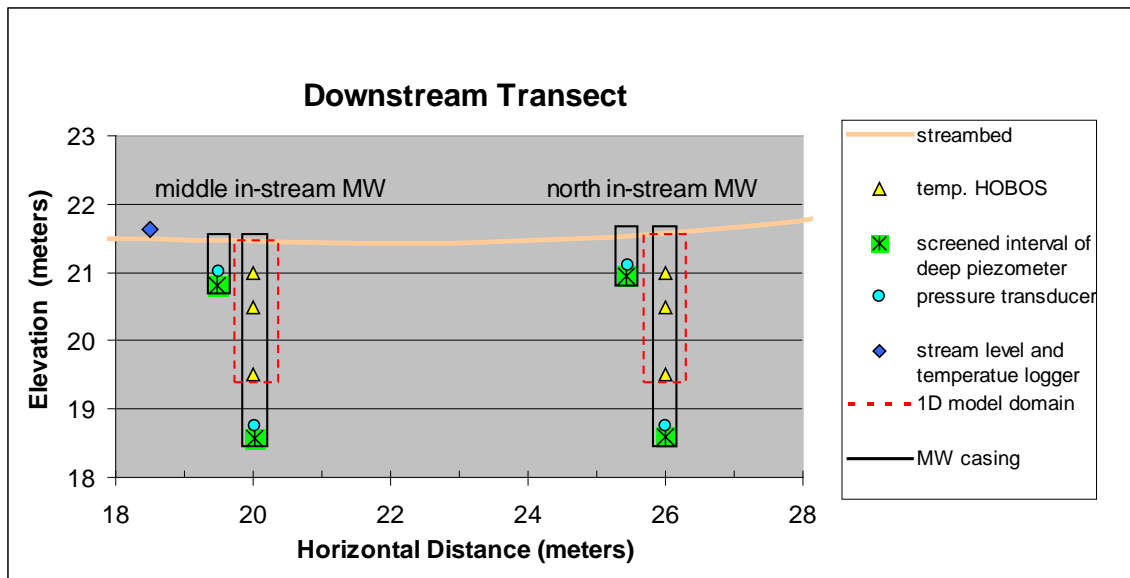
Figure 21. Cross-section for downstream transect showing measurement locations and model domain.

Flux estimates from heat and water flow modeling were not conducted at the upstream

transect due to limited quantity and quality of temperature and total head data. The

energy transport and water flow model, VS2DH, was used to fit simulated temperatures

to observed temperatures and heads. It is important to note that due to problems with the

measured stream elevations as discussed in the total head distribution section, stream

elevation was not used as the top boundary condition. Instead, a value of zero pressure

head (rather than total pressure head) was assigned to the top boundary for the model (at

the sediment/water interface) and the difference in pressure head between the deep and

shallow wells was assigned to the bottom boundary for the model. Therefore, a positive

pressure head indicates upward flow through the model domain to the sediment/water

interface and a negative pressure head indicates a downward flow through the model

domain.

Figure 21 depicts the model domain at 2 meters below the streambed, with a

lower model boundary that corresponds to the deepest temperature logger; however, the

screened interval of the MW is at 3 meters below the streambed. As a result, the head

difference between a deep and shallow well is over a vertical distance of 2.5 meters

(pressure head in MW screened at 3 m below streambed – pressure head in MW screened

at 0.5 m) and does not match the model domain. It was assumed that the measured head

difference over 2.5 meters was linear and that the hydraulic conductivity (K) of the

materials throughout the model domain was constant due to the homogenous streambed

material. Therefore, the head difference over 2.5 meters was corrected to a head

difference over 2 meters to match the model domain. The temperatures applied to the top

and bottom boundaries were recorded temperature in the stream and 2 meters below the streambed, respectively. Estimates of streambed hydraulic input into the model until model simulations provided a "best fit" of observed temperatures at depth. The observed temperature used to match model simulations were measured were 0.5 and 1.0 meters below the streambed. Figures 22 and 23 depict the results of the 1D modeling efforts at the downstream transect for the north and middle in-stream monitoring wells, respectively.

The streambed of the lower Merced Basin proved to be a highly dynamic system, with mobile bar forms and substantial bed load transport during periods of low streamflow (observed during measurements with seepage meters). High streamflow events also included suspended load. The model results in figures 22 and 23 depict periods where simulated temperatures nearly match observed temperatures. Periods of departure have three explanations: (1) they may be the result of the streambed characteristics changing over time resulting in varying K values; (2) they may be a result of scour near wells that changes the effective depth of the temperature loggers and alters the model domain; and (3) the hydraulic head gradient the model calculates is over a 2 m domain, however, changes in effective depth of pressure transducers due to scour near wells may not always coincide with the assumed model domain, resulting in calculated head gradients that are not representative of actual gradients.
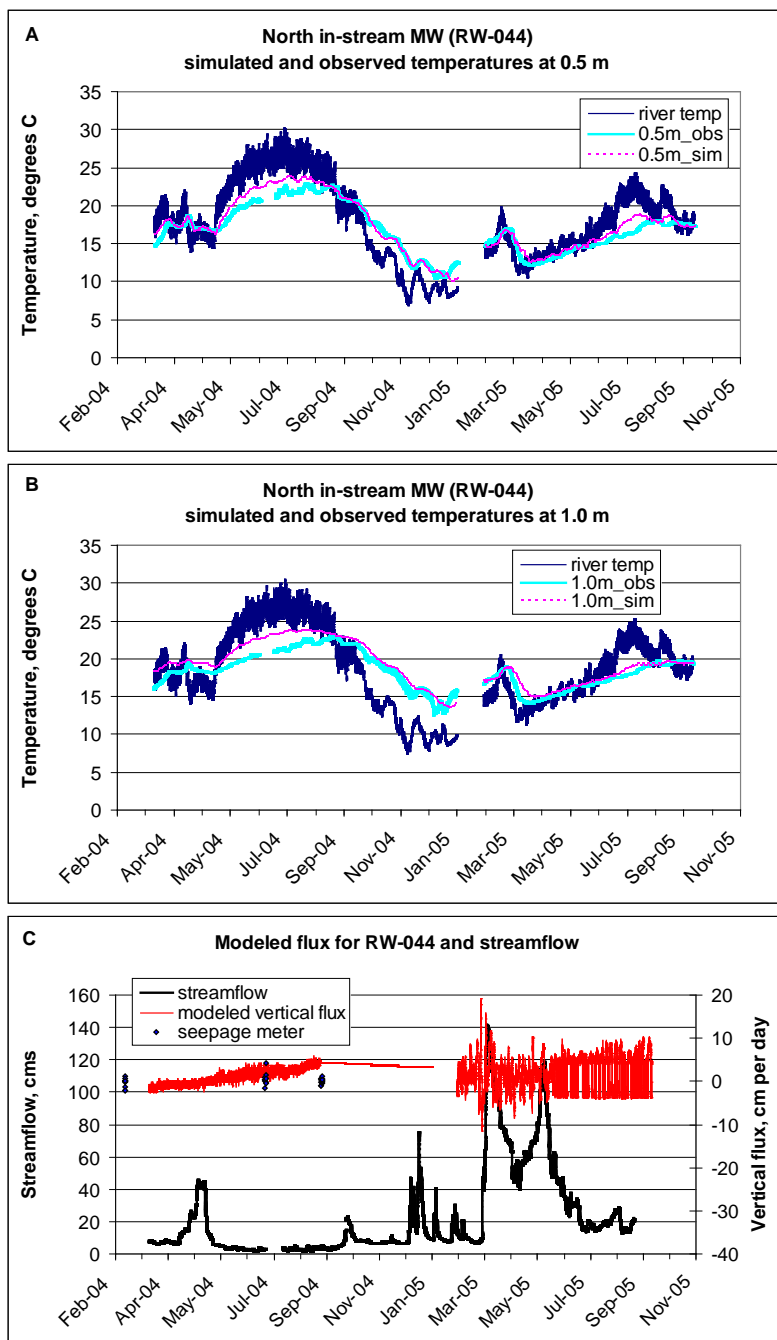
Figure 22. Plots of observed and simulated temperatures for the north in-stream MW at (**A**) 0.5 meters, (**B**) 1.0 meter, and (**C**) modeled vertical flux, seepage meter measurements and streamflow.
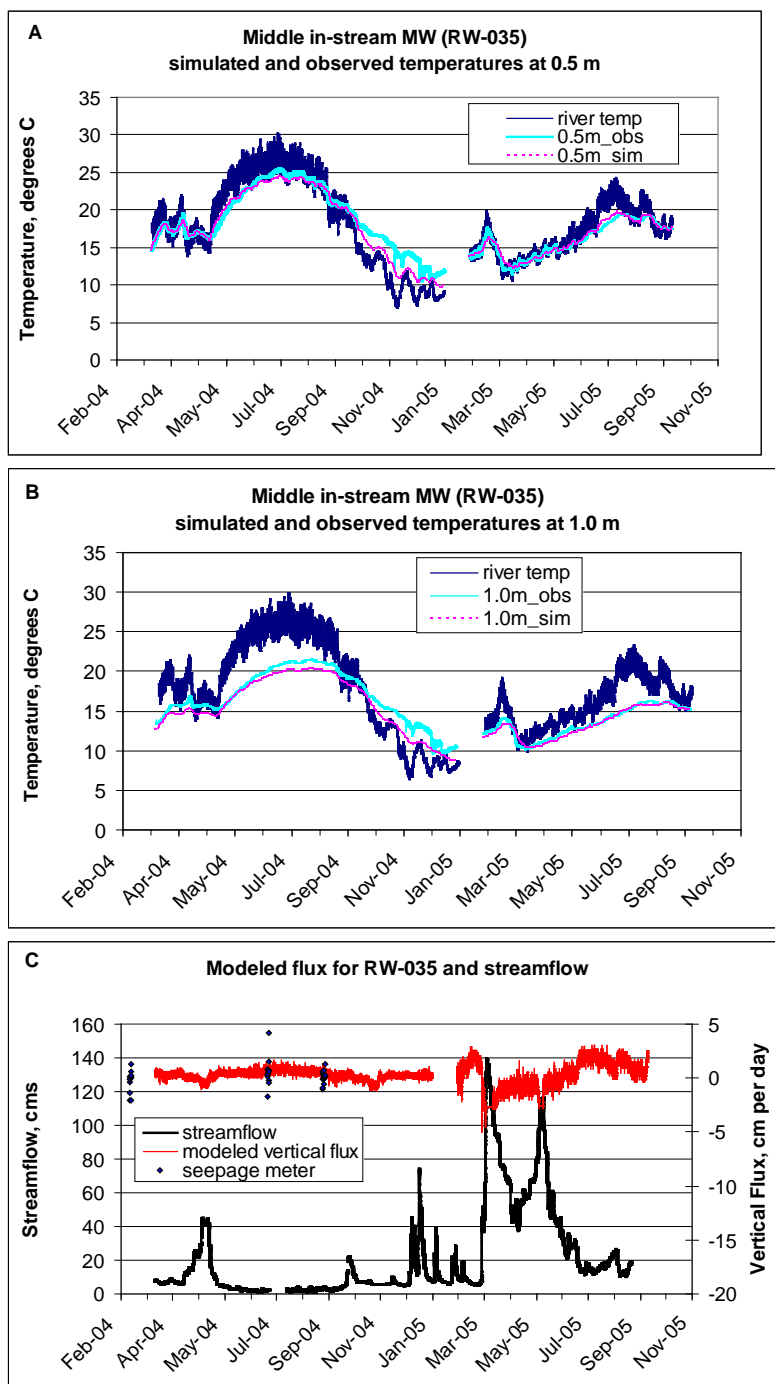
Figure 23. Plots of observed and simulated temperatures for the middle in-stream MW at (**A**) 0.5 meters, (**B**) 1.0 meter, and (**C**) modeled vertical flux, seepage meter measurements and streamflow.

An example of a departure from observed temperatures occurs in the middle in-stream well (figure 23) following the dam release in October 2004. The simulated and observed temperatures at 0.5 and 1.0 meter match well up until the dam release, but depart during and following the release. The higher streamflow likely scoured out the fines accumulated over the summer prior to the October release thereby increasing the streambed K.

The departure of simulated temperatures from observed temperatures for this time period indicates that in order for the simulated to continue to match the observed, the streambed K (and resultant vertical flux) must be higher than the model input value used prior to this period. Figure 24 depicts the results of a model run in which the streambed K was increased from 1 m/day to 3 m/day for the period of departure. The resultant simulated temperatures for the departure period provide an improved match to observed temperatures and substantiate the interpretation for this departure. The resultant modeled vertical flux increased from 0.4 cm/day to 4.6 cm/day.
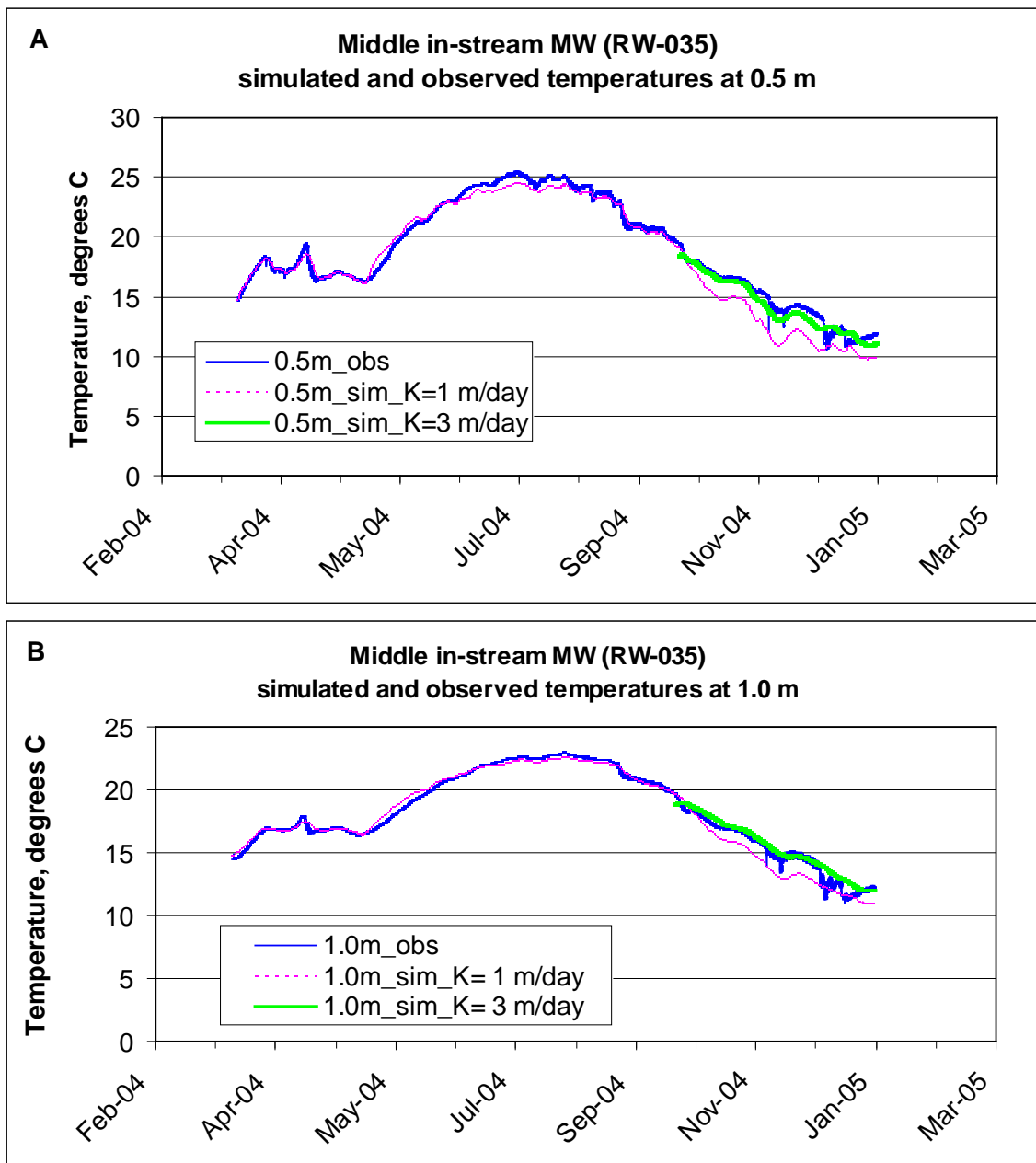
Figure 24. Results of simulated temperatures with an increase in hydraulic conductivity beginning at departure**.**

Although increasing hydraulic conductivity improves the simulated to observed temperatures; it is difficult to accept that this factor alone explains the departure as it unlikely that vertical flux increased an order of magnitude over a short period of time. Instead, a combination of factors may better explain the departure. It is likely that changes in effective depth of pressure transducers due to scour near wells resulted in instrumentation depth not coinciding with the assumed model domain. The result is that head gradients the model calculates are not representative of actual gradients. This explanation coupled with increased streambed K due to scouring of fines due to higher streamflow may provide a more accurate explanation of the departure.

Due to the data gap that occurs between January and February 2005 for both wells, the models for each well depicted in figures 22 and 23 were run as two parts (part 1 and part 2). Table 8 lists the input values of hydraulic, thermal conductivity, and average vertical flux for model parts 1 and 2. Results from RW-035 (the middle in-stream well) uses a slightly higher K value for the second part of the model, and correspond to the same value used to match the departure in figure 24 (3.0 m/day). Although the streambed K was increased from 1m/day to 3m/ day in part 2, the average vertical flux only increased from 0.4 cm/day to 0.5cm/day. This is explained by the large range of streamflow that occurred during this time period. High streamflow events result in flow reversals, and the average vertical flux takes into account gaining, losing, and neutral values.

Table 8. Modeling input values of listed parameters for modeling parts 1 and 2.

Well Location	Well Name	Thermal Conductivity (W/m ºC)	Hydraulic Conductivity (m/day)	Average Vertical Flux (cm/day)
North in-stream well, part 1	RW-044	1.8	2.6	2.2
North in-stream well, part 2		1.8	2.6	2.2
Middle in-stream monitoring well, part 1	RW-035	1.8	1.0	0.4
Middle in-stream monitoring well, part 2		1.8	3.0	0.5

The departures that occurred in part 1 of the north in-stream monitoring well (figure 22) are also likely a result of the changing streambed K, however cannot explain departures observed in part 2.   It was expected that the K would also increase following high streamflow events as they did for the middle in-stream well, however this was not the case as the same K value was used for parts 1 and 2 (table 8). This may be a result of the variability or "noise" in recorded pressure head values (figure 18a), or effects on the model domain due to scour around the monitoring wells. Another possible explanation may be river geomorphology. The downstream transect is located across a moderate meander with the location of the depositional side occurring at the north in-stream monitoring well pair and the erosional side occurring on the south cut bank. The north in-stream monitoring well is therefore subject to constant deposition due to the helical flow occurring around the meander bend. This corkscrew motion promotes scouring along the bottom toward the cut bank and deposition on the opposite bank at the location of the north in-stream monitoring wells. As a result, it is unclear if the calculated average flux value is representative for part 2 of this model.

CONCLUSIONS

Estimates of vertical flux across the sediment/water interface were made by direct measurement using seepage meters and heat as tracer in a 100 m reach of the lower Merced River. Results of the temperature modeling efforts indicate that the Merced River at the study reach is generally a slightly gaining stream with very small head differences between surface water and ground water, and flow reversals occurring during high streamflow events. The period of study included a large range of streamflow that affected the streambed characteristics and hydraulic conductivity of the streambed. The high streamflow events associated with storm run-off events and large releases at the upstream dam resulted in an increase in hydraulic conductivity due to the scouring of fines accumulated during periods of low streamflow. The average vertical flux across the sediment/water interface for the study period was 0.4-2.2 cm/day and the range of hydraulic conductivities was 1-3 m/day at the study reach.

The use of seepage meters to directly measure vertical flux generally failed in this high-energy system due to slow seepage rates and a mobile streambed that scoured or buried the seepage meters. Estimates of streambed K made by grain size analysis methods and slug tests generally showed close agreement. The arithmetic mean of these methods resulted in hydraulic conductivities ranging from approximately 45-220 m/day at the upstream transect and 20-150 m/day at the downstream transect.

SUGGESTIONS FOR FUTURE STUDIES

A significant conclusion that came from applying heat as a tracer to estimate vertical flux across the sediment/water interface was the importance of maintaining vertical control on the elevations of instrumentation used to record hydraulic pressure heads. This is especially important in settings where the hydraulic head differences between surface water and ground water are very slight. In this study, un-vented pressure transducers coupled with a barometer were used to record hydraulic pressure head. The application of this instrumentation proved to be problematic. Un-vented pressure transducers will often have more error associated with recorded water level data than the differences in water levels themselves and measured values tend to drift over time. Thus, it is recommended that high-precision vented pressure transducers be used in these settings where differences in hydraulic head between the surface water and ground water are slight. One of the initial objectives of this study was to model temperature in 1-dimension and 2-dimensions across a transect. However, due to poor vertical control on stream elevation coupled with the type of pressure transducers used, the 2-dimensional modeling was not accomplished.

APPENDIX

Sampling Event 1. December 2-4, 2003

Seepage Meter	Bag type	vertical seepage rate (cm/day)	vertical seepage rate (cm/day)
		December 2-3, 2003	December 3-4, 2003
A	shower bag	0.01	-0.5
1	medical bag	-1.51	-1.13
B	shower bag	-0.16	0.11
2	medical bag	-2.12	-1.06
C	shower bag	0.24	0.2
3	medical bag	lost stopper	0.5
D	shower bag	0.02	0.16
4	medical bag	-1.49	-1.71
E	shower bag	0.07	0.15
5	medical bag	-0.06	1.23
F	shower bag	-0.48	-0.08
6	medical bag	0.19	-0.48

Sampling Event 2. January 29-31, 2004

Seepage Meter	Bag type	vertical seepage rate (cm/day)	vertical seepage rate (cm/day)
		January 29-30, 2004	January 30-31, 2004
A	shower bag	0.05	-0.06
1	medical bag	0.19	0.89
B	shower bag	0.21	0.24
2	medical bag	-0.57	0.13
C	shower bag	0.15	0.15
3	medical bag	-1.23	-1.9
D	shower bag*	0.15	-0.01
4	medical bag*	-0.03	-1.87
E	shower bag*	0.14	complete scour of meter
5	medical bag*	-1.73	-2.2
F	shower bag*	0.18	-0.43
6	medical bag*	-0.23	-1.94

[*indicates shower bag or medical bag used in the first 24 hour measurement period and packaging bag used in the second 24 hour measurement]

Sampling Event 3. February 10-12, 2004

Seepage Meter	Bag type	vertical seepage rate (cm/day)	vertical seepage rate (cm/day)
		February 10-11, 2004	February 11-12, 2004
A	shower bag	0.2	0.17
1	medical bag	0.83	0.17
B	shower bag	0.07	-0.02
2	medical bag	-2.09	-2.05
C	shower bag	0.18	0.01
3	medical bag	0.03	-0.79
D	shower bag*	-0.03	0.02
4	medical bag*	-1.35	-2.02
E	shower bag*	0.13	0.11
5	medical bag*	-2.04	1.32
F	shower bag*	-0.04	0.56
6	medical bag*	-0.07	0.20

[*indicates shower bag or medical bag used in the first 24 hour measurement period and packaging bag used in the second 24 hour measurement]

Sampling Event 4. July 19-21, 2004

Seepage Meter	Bag type	vertical seepage rate (cm/day)	vertical seepage rate (cm/day)
		July 19-20, 2004	July 20-21, 2004
A	packaging bag	0.43	0.61
1	packaging bag	-1.33	0.45
B	packaging bag	0.46	-0.1
2	packaging bag	-1.57	4.3
C	packaging bag	0.38	0.71
3	packaging bag	2.78	4.19
D	packaging bag	0.39	-0.23
4	packaging bag	-1.68	1.51
E	packaging bag	0.11	0.75
5	packaging bag	housing unit dislodged	4.15
F	packaging bag	0.35	0.57
6	packaging bag	0.79	-0.41

Sampling Event 5. September 20-22, 2004

Seepage Meter	Bag type	vertical seepage rate (cm/day)	vertical seepage rate (cm/day)
		September 20-21, 2004	September 21-22, 2004
A	packaging bag	0.31	0.25
1	packaging bag	-0.16	-0.11
B	packaging bag	collection bag disconnected	0.24
2	packaging bag	-1.13	-0.63
C	packaging bag	-0.05	0.52
3	packaging bag	-1.13	-0.23
D	packaging bag	hole developed in collection bag	0.4
4	packaging bag	-1.01	-0.55
E	packaging bag	0.6	-0.11
5	packaging bag	-0.14	0.77
F	packaging bag	0.43	0.03
6	packaging bag	-0.9	0.12

Sampling Event 6. September 22-23, 2004

Seepage Meter	Bag type	vertical seepage rate (cm/day) September 21-22, 2004	vertical seepage rate (cm/day) September 22-23, 2004
A	packaging bag	0.25	0.14
1	packaging bag	-0.11	0.46
B	packaging bag	0.24	0.11
2	packaging bag	-0.63	1.04
C	packaging bag	0.52	0.06
3	packaging bag	-0.23	-1.2
D	packaging bag	0.4	0.12
4	packaging bag	-0.55	1.29
E	packaging bag	-0.11	0.27
5	packaging bag	0.77	0.8
F	packaging bag	0.03	-0.15
6	packaging bag	0.12	-0.4

REFERENCES CITED

Alyamani, M.S. and Sen, Z., 1993, Determination of hydraulic conductivity from complete grain-size distribution curves: Ground Water, v. 30, no. 4, 551-555.

Anderson, M.P., 2005, Heat as a ground water tracer: Ground Water, v. 46 (6), p. 951-968

Ashbury, C.E., 1990, The role of groundwater seepage in sediment chemistry and nutrient budgets in Mirror Lake, New Hampshire: PhD thesis, Cornell University

Bartolino, J. and Niswonger, R., 1999, Temperature profiles of the aquifer system underlying the Rio Grande, NM, Proceedings of Third Annual Middle Rio Grande Basin Workshop, Feb 22-23,1999: U.S. Geological Survey Open-File Report 99-203, p. 66-67.

Bartow, J.A., 1991, The Cenozioc evolution of the San Joaquin Valley, California: U.S. Geological Survey Professional Paper 1501, 40 p.

Belanger, T.V. and Mikutel, D.F., 1985, On the use of seepage meters to estimate ground water nutrient loading to lakes: Water Resources Bulletin, v. 21, p. 265-271.

Belanger, T.V. and Montgomery, M.T., 1992, Seepage meter errors: Limnology and Oceanography v. 37, no. 8, p. 1787-1795.

Blanchefield, P.J., and Ridgeway, M.S., 1996, Use of seepage meters to measure ground water flow at brook trout redds: Transactions of American Fishery Society, v. 125 p. 813-818.

Brunke, M., and Gonser, T., 1997, The ecological significance of exchange processes between rivers and ground water: Freshwater Biology, 37, p.1-33.

Bouwer, H., and Rice, R.C., 1976, A slug test method for determining hydraulic conductivity of unconfined aquifers with completely or partially penetrating wells: Water Resources Research, vol. 12, no.3, p. 423-428.

Boyle, D.R., 1994, Design of a seepage meter for measuring ground water fluxes in the nonlittoral zone of lakes─Evaluation in a boreal forest lake: Limnology and Oceanography, v. 39, p. 670-681.

Bravo, H.R., Feng, J., and Hunt, R.J., 2002, Using ground water temperature data to constrain parameter estimation in a ground water flow model of a wetland system: Water Resources Research 38, no. 8, p.

Brock, T.D., Lee D.L., Janes, D.,and Winek, D., 1982, Ground water seepage as a nutrient source to a drainage lake, Lake Mendota, Wisconsin: Water Resources, v. 16, p. 1255-1263.

Burow, K.R., Shelton, J.L., Hevesi, J.A., Weismann, G.S., 2004, Hydrogeologic characterization of the Modesto area, San Joaquin Valley, California: U.S. Geological Survey Scientific Investigation Report 2004-5232, 54 p.

Cable, J.E., Burnett, W.C., Chanton, J.P., Corbett, D.R., and Cable P.H., 1997, Field evaluation of seepage meters in the coastal marine environment: Estuarine and Coastal Shelf Science, v. 45, p. 367-375.

Cardenas, M.B., and Zlotnik, V.A., 2003, A simple constant-head injection test for streambed hydraulic conductivity estimation: Ground Water, vol. 41, no. 6, p. 867-871.

Cey, E.E., Rudolph, D.L., Parkin, G.W., and Aravena, R., 1998, Quantifying ground water discharge to a small perennial stream in southern Ontario, Canada: Journal of Hydrology, v. 210, p. 21-37.

Chanton, J.P., Burnett, W.C., Dulaiova, H., Corbett, D.R., and Taniguchi, M., 2003, Seepage rate variability in Florida Bay drive by Atlantic tidal height: Biogeochemistry, v. 66. p. 187-202.

Cherkauer, D.A, and J.M. McBride, 1988, A remotely operated seepage meter for use in large lake and rivers: Ground water v. 26, p. 165-171

Choi, J., and Harvey, J.W., 2000, Quantifying time-varying ground-water discharge and recharge in wetlands of the northern Florida Everglades: Wetlands, v. 20, p. 500-511.

Connor, J.N., and Belanger, T.V., 1981, Ground water seepage in Lake Washington and the Upper St. Johns Basin, Florida: Water Resources Bulletin, v. 17, p. 799-805.

Conrad, L.P., and Beljin, M.S., 1996, Evaluation of an induced infiltration model as applied to glacial aquifer systems: Water Resources Bulletins 32, no. 6, p. 1209-1220.

Constantz, J., and Thomas, C.L., 1997, Streambed temperature profiles as indicators of percolation characteristics beneath Arroyos in the Middle Rio Grande Basin, USA: Hydrological Processes, v. 11, p. 1621-1634.

Constantz, J., 1998. Interaction between stream temperature, streamflow, and ground water exchanges in alpine streams: Water Resources Research, v. 34, no. 7, p. 1609-1615.

Constantz, J., Stonestrom, D., Stewart, A.E., Niswonger, R., and Smith, T.R., 2001, Analysis of streambed temperatures in ephemeral channels to determine streamflow frequency and duration: Water Resources Research, v. 37, no. 2, p. 317-328.

Constantz, J., Stewart, A.E., Niswonger, R., and Sarma, L., 2002, Analysis of temperature profiles for investigating stream losses beneath ephemeral channels: Water Resources Research, v. 38, no. 12, p. 52-1 to 52-13.

Croft, M.G., 1972, Subsurface geology of the late Tertiary and Quaternary water-bearing deposits of the southern part of the San Joaquin Valley, California: U.S. Geological Survey Water-Supply Paper 1999-H, 29 p.

Davies, W.J., 2002, Evaluation of Diver Water-Sensor and Baro Diver Sensor, USGS Water Resources Discipline Instrument News, issue 98, p. 11- 18. http://wwwhif.er.usgs.gov/uo/pubs/wrdin/Sept2002.pdf

Davis, S.N., and Hall, F.R., 1959, Water-quality of the eastern Stanislaus and northern Merced counties, California: Stanford University Publications, Geological Sciences, v. 6, no. 1, 112 p.

Davis, S.N., and DeWiest, R.J.M., 1966, Hydrogeology, John Wiley & Sons, New York, NY.

Downing, J.A., and Perterka, J.J., 1978, The relationship of rainfall and lake ground water seepage: Limnology and Oceanography, v. 23, p. 821-825.

Dumouchelle, D.H., 2001, Evaluation of Ground-Water/Surface-Water Relations, Chapman Creek, West-Central Ohio, by means of multiple methods: USGS Water Resources Investigative Report 01-4202. 13 p.

Duwelius, R.F., 1996, Hydraulic conductivity of the streambed, East Branch Grand Calumet River, Northern Lake County, Indiana. U.S. Geological Survey Water-Resources Investigations Report 96-4218.

Erickson, D.R., 1981, A study of littoral ground water seepage at Williams Lake, Minnesota using seepage meters and wells: M.S. thesis, University of Minnesota, 153 p.

Fetter, C.W., 2001, Applied Hydrogeology: New York, NY, Macmillan College Publishing Company, 598 p.

Fellows, C.R., and Brezonik, P.L., 1980, Seepage flow into Florida Lakes: Water Resources Bulletin, v. 16, p. 635-641.

Findlay, S. 1995, Importance of surface-subsurface exchange in stream ecosystems: the hyporheic zone: Limnology and Oceanography 40(1), p. 159-164.

Freeze, R.A., and Cherry, J.A., 1979, Ground water: Engelwood Cliffs, N.J., Prentice-Hall, 604 p.

Fryar, A.E., Wallin, E.J., and Brown, D.L., 2000, Spatial and temporal variability in seepage between a contaminated aquifer and tributaries to the Ohio River: Ground water Monitoring Remediation, v. 20, p. 129-146.

Gilbert J., Danielopol, D.L., and Stanford, J.A., 1994, Ground water Ecology: San Diego, CA, Academic Press, 571pp.

Hantush, M.S., 1965, Wells near steram with semipervious beds: Journal of Geophysical Research 70, no. 12, p. 2829-2838.

Harleman, D.R.F., Melhorn, P.F., and Rumer, R.R., 1963, Dispersion-permeability correlation in porous media: American Society of Civil Engineers, v. 89, p. 67-85.

Hart, D.R., Mulholland, P.J., Marzolf, D.L., DeAngelis, D.L., and Hendricks, S.P., 1999, Relationships between hydraulic parameters in a small stream under varying flow and seasonal conditions: Hydrological Processes 13, no. 10, p. 1497-1510.\

Harvey, F.E., and Lee, D.R., 2000, Discussion of "The effects of bag type and meter size on seepage meter measurements": Ground water, v. 38, p. 326-328.

Harvey, J.W., and Bencala, K.E., 1993, The effect of streambed topography on surface-subsurface water exchange in mountain catchments: Water Resources Research 29, no. 1, p. 89-98.

Harvey, J.W., and Wagner, B.J., 2000, Quantifying hydrologic interactions between steams and their subsurface hyporheic zones *in* Streams and Ground waters: New York, NY, Academic Press, p. 3-44.

Hazen, A., 1911, Discussion: Dams of sand foundations: Transactions, American Society of Civil Engineers, 73:1999

Healy, R.W., and Ronan, A.D., 1996, Documentation of computer program VS2DH for simulation of energy transport in variably saturated porous media─modification of the U.S. Geological Survey Water-Resources Investigations Report 96-4230, 36p. An electronic version of this report can be downloaded from: http://pubs.er.usgs.gov/pubs/wri/wri964230

Hsieh, P.A., Wingle, W., and Healy, R.W., 2000, VS2DI─A graphical software package for Simulating Fluid Flow and Solute or Energy Transport in Variably Saturated Porous Media: U.S. Geological Survey Water-Resources Investigations Report 99-4130, 16 p.

Hunt, B., 1999, Unsteady stream depletion from ground water pumping: Ground Water 37, no. 1, pg. 98-102.

Hvorslev, M.J., 1951, Time lag and soil permeability in ground-water observations: Vicksburg, Miss., U.S. Army Waterways Experiment Station, Corps of Engineers Bulletin no. 36, 49 p.

HydroSOLVE, Inc., 2003, AQTESOLV for Windows version 3.5, Reston, VA

Isiorho, S.A., and Meyer, J.H., 1999, The effects of bag type and meter size on seepage meter measurements: Ground water, v. 37, no. 3, p. 411-413.

Isiorho, S.A., and Matisoff, G., 1990, Ground water recharge from Lake Chad: Limnology and Oceanography, v. 35, p. 931-938.

Israelsen, O. W., and R.C., Reeve, 1944, Canal lining experiments in the Delta Area: Utah Tech. Bull. 313, Utah Agric. Exp. Stn., Logan.

Jackman, A.P., Triska, F.J. and Duff J.H., 1997, Hydrologic examination of ground water discharge into the upper Shingobee River: USGS Water Resources Investigative Report 96-4215, p. 137-147.

John, P.H., and Lock, M.A., 1977, The spatial distribution of ground water discharge into the littoral zone of a New Zealand Lake: Journal of Hydrology, v. 33 p. 391-395

Kelly, S.E., 2001, Methods for determining the hydrologic characteristics of stream beds: M.S. thesis, Clemson University, 111 p.

Kelly, S.E., and Murdoch, L.C., 2003, Measuring the hydraulic conductivity of shallow submerged sediments: Ground water, vol. 41, no. 4, p. 431-439.

Krumbein, W.C., and Monk, G.D., 1942, Permeability as a function of the size parameters of unconsolidated sand: Transactions of the American Institute of Mining and Metallurgical Engineers v. 151, p. 153-163

Landon, M.K., Rus, D.L., and Harvey, F.E., 2001, Comparison of in-stream methods of measuring hydraulic conductivity in sandy streambeds: Ground Water, v. 39, p. 870-885.

Lapham, W.W., 1988, Conductive and convective heat transfer in sediments near streams: Tucson, Ariz., University of Arizona, Ph. D. dissertation, 315 p.

Lapham, W.W., 1989, Use of temperature profiles beneath streams to determine rates of vertical ground-water flow and vertical hydraulic conductivity: U.S. Geological Survey Water-Supply Paper 2337, 35 p.

Larkin, R.G. and J.M. Sharp, 1992, On the relationship between river-basin geomorphology, aquifer hydraulics, and ground-water flow direction in alluvial aquifers. Geological Society of America Bulletin 104, no. 12, p. 1608-1620.

Lee, D.R., 1977, A device for measuring seepage flux in lakes and estuaries: Limnology and Oceanography, v.22, p. 140-147.

Lee, D.R., and Cherry, J.A., 1978, A field exercise on ground water flow using seepage meters and mini-piezometers: Journal of Geology Education, v. 27, p. 6-10.

Lee, D.R., and Hynes H.B., 1977, Identification of ground water discharge zones in a reach of Hillman Creek in Southern Ontario: Water Pollution Resources Canada, v. 13, p. 121-133.

Lesack, L.F., 1995, Seepage exchange in an Amazon floodplain lake: Limnology and Oceanography, v. 40, p. 598-609.

Libelo, L.E., and MacIntyre, W.G., 1994, Effects of surface-water movement on seepage meter measurements of flow through the sediment-water interface: Applied Hydrogeology, v. 4, p. 49-54.

Linderfelt, W.R., and Turner, J.V., 2001, Interaction between shallow ground water, saline surface water and nutrient discharge in a seasonal estuary: the Swan-Canning system: Hydrological Processes, v. 15. p. 2631-2653.

Lindgren, R.J., and Landon, M.K., 2000, Effects of ground-water withdrawals on the Rock River and associated valley aquifer, Eastern Rock County, Minnesota: U.S. Geological Survey Water-Resources Investigations Report 99-4157.

Lock, M.A., and John, P.A., 1978, The measurement of ground water discharge into a lake by a direct method, International Review of Hydrobiology, v. 63, p 271-275.

Masch, F.D., and Denny, K.T., 1966, Grain-size distribution and its effect on the permeability of unconsolidated sands: Water Resources Research, v. 2, p. 665-677.

McBride, J.M., 1987, Measurement of ground water flow to the Detroit River, Michigan and Ontario: MS thesis, University of Wisconsin-Milwaukee.

McMahon, P.B., Tindall, J.A., Collins, J.A., Hull, K.J., and Nuttle, J.R., 1995, Hydrologic and geochemical effects on oxygen uptake in bottom sediments of an effluent-dominated river: Water Resources Research 31, no.10, p. 2561-2569.

Modesto Irrigation District, Water and Power, 2005, Precipitation and temperature data for 1988-2005 for Modesto, <URL http://www.mid.org/wthr/html>Data obtained from customer service (OR written communication Kate Hora).

Murdoch, L.C., and Kelly, S.E., 2003, Factors affecting the performance of conventional seepage meters: Water Resources Research, v.39, no. 6.

Page, R.W., 1977, Appraisal of ground-water conditions in Merced, California, and vicinity: U.S. Geological Survey Open-File Report 77-454, 43 p.

Page, R.W., 1986, Geology of the fresh ground-water basin of the Central Valley, California, with texture maps and sections: U.S. Geological Survey Professional Paper 1401-C, 54 p., 5 pls in pocket.

Page, R.W., and Balding, G.N., 1973, Geology and quality of water in the Modesto-Merced area, San Joaquin Valley, California: U.S. Geological Survey Water Resources Investigations Report 73-6, 85 p.

Paulsen, R.J., Smith, C.F., O'Rourke, D., and Wong, T.F., 2001, Development and evaluation of an ultrasonic ground water seepage meter: Ground water, v. 39, p. 904-911.

Rorabaugh, M.I., 1954, Streambed percolation in development of water supplies, U.S. Geological Survey Ground water Notes on Hydraulics No. 25, 13 p.

Rosenberry, D.O, 2005, Integrating seepage heterogeneity with the use of ganged seepage meters, Limnology and Oceanography: Methods, 3, p. 131-142.

Rosenberry, D.O., 2000, Unsaturated-zone wedge beneath a large, natural lake: Water Resources Research, v. 36, p. 3401-3409.

Rosenberry, D.O., and Morin, R.J., 2004, Use of an Electromagnetic Seepage Meter to Investigate Temporal Variability in Lake Seepage: Ground water, v. 41, p. 68-77.

Schincariol, R.A., and McNeil, J.D., 2002, Errors with small volume elastic seepage bags: Ground water, v. 40, p. 649.

Sebestyen, S.D., and Schneider, R.L., 2001, Dynamic temporal patterns of nearshore seepage flux in headwater Adirondack lake: Journal of Hydrology, v. 247, p. 137-150.

Shaw, R.D., and Prepas, E.E., 1989, Anomalous, short-term influx of water into seepage meters: Limnology and Oceanography, v. 34, no.7, p. 1343-1351.

Shaw, R.D., and Prepas, E.E., 1990a, Ground water-lake interactions: I. Accuracy of seepage meter estimates of lake seepage: Journal of Hydrology, v 119, p. 105-120.

Shaw, R.D., and Prepas, E.E., 1990b, Ground water-lake interactions: II. Nearshore seepage patterns and the contribution of ground water to lakes in central Alberta: Journal of Hydrology, v. 112, p. 121-136.

Shaw, R.D., Shaw, J.F.H., Fricker, H., and Prepas, E.E., 1990, An integrated approached to quantify ground water transport of phosphorus to Narrow Lake, Alberta: Limnology and Oceanography, v. 35, p. 870-886.

Shepard, R.G., 1989, Correlations of permeability and grain size: Ground Water, v. 22, no. 5, p. 633-638.

Shinn, E.A., Reich, C.D., and Hickey, T.D., 2002, Seepage meters and Bernoulli's Revenge: Estuaries, v. 25, p. 126-132.

Silliman, S.E., and Booth, D.F., 1993, Analysis of time-series measurements of sediment temperature for identification of gaining vs. losing portions of Juday Creek, Indiana: Journal of Hydrology, v. 146, p. 131-148.

Silliman, S.E., Ramirez, J., and McCabe, R.L., 1995, Quantifying downflow through creek sediments using temperature time series; one-dimensional solution incorporating measured surface temperature: Journal of Hydrology, v. 167, p. 99-119.

Sorey, M.L., 1971, Measurement of vertical ground water velocity from temperature profiles in a well: Water Resources Research, v. 7, p. 963-970.

Springer, A.E., Pertroutson, W.D., and Semmens, B.A., 1999, Spatial and temporal variability of hydraulic conductivity in active reattachment bars of the Colorado River, Grand Canyon: Ground Water 37, no. 3, p. 338-344.

Stallman, R.W., 1963, Methods of collecting and interpreting ground-water data, U.S. Geological Survey Water-Supply Paper 1544-H, p. 36-46.

Stillwater Sciences and EDAW Inc., 2001, Merced River Corridor Restoration Plan Baseline Studies, Vol. I: Identification of Social, Institutional and Infrastructural Opportunites and Constraints, Final Report.

Stonestrom, D.A., and Constantz, J., eds., 2003, Heat as a Tool for Studying the Movement of Ground Water Near Streams: U.S. Geological Survey Circular 1260, 96 p.

Stonestrom, D.A., and Constantz, J., 2004, Using temperature to study stream-ground water exchanges: U.S. Geological Survey Fact Sheet 2004-3010

Su, G.W., Jasperse, J., Seyour, D., and Constantz, J., 2004, Estimation of hydraulic conductivity in an alluvial system using temperature: Ground Water, vol. 42, no. 6, p. 890-901.

Suzuki, S., 1960, Percolation measurements based on heat flow through soil with special reference to paddy fields: Journal of Geophysical Research, v. 65, p. 2883-2885.

Taniguchi, M., 2002, Tidal effects submarine groundwater discharge into the ocean: Geophys. Res. Lett. 29

Taniguchi, M. and Fukuo, Y.,1993, Continuous measurements of ground water seepage using a automatic seepage meter: Ground water, v. 31, no.7, p. 675-679.

Todd, D.K., 1980, Ground water Hydrogeology. John Wesley & Sons Inc., New York, NY. 535 p.

Vogelmann, J.E., Howard, S.M., Yang, L., Larson, C.R., Wylie, B.K., and Van Driel, N., 2001, Completion of the 1990s National land cover data set for the conterminous United States fro Landsat Tematic Mapper data and ancillary data sources, Photogrammetric Engineering and Remote Sensing 67: 650-652.

Weibenga, W.A., Ellis, W.R., and Kevi, L., 1970, Empirical relations in properties of unconsolidated quartz sands and silts pertaining to water flow: Water Resources Research, v. 6, p. 1154-1161.

Winter, T.C., Harvey, J.W., Franke, O.L., and Alley, W.M., 1998, Ground water and surface water, a single resource, U.S. Geological Survey Circular 1139, 79 p.

Woessner, W.W., and Sullivan, K.E., 1984, Results of seepage meter and mini-piezometer study, Lake Mead, Nevada: Ground Water, v. 22, p. 561-568.

Wolf, S.H., Celia, M.A., and Hess, K.M., 1991, Evaluation of hydraulic conductivities calculated from multiport-permeameters measurements: Ground Water 29, no. 4, p. 516-525.

Wrobickly, G.L, Campana, M.E., Vallet, H.M., and Dahm, C.N., 1998, Seasonal variation in surface-subsurface water exchange and lateral hyporheic area of two stream-aquifer systems: Water Resources Research, v. 34, no. 3, p. 317-32.

Yager, R.M., 1993, Estimation of hydraulic conductivity of a riverbed and aquifer system on the Susquehanna River in Broome County, New York. U.S. Geological Survey Water-Supply Paper 2387.

Yelverton, G.F., and Hackney, C.T., 1986, Flux of dissolved organic carbon and pore water through the substrate of a *Spartina alterflora* marsh in North Carolina: Estuarine and Coastal Shelf Scienc, v. 22, p. 255-267.

Zimmerman, C.F., Montgomery, J.R., and Carlson, P.R., 1985, Variability of dissolved reactive phosphate flux rates in near shore estuarine sediments: effects of ground water flow: Estuaries, v. 8, p. 228-236.